The Response of Composite Materials Subjected to Underwater Explosive Loading: Experimental and Computational Studies

James LeBlanc, Erin Gauch, Carlos Javier, and Arun Shukla

1 Introduction

Within many marine industries there is a significant and increased interest in the use of composite materials to support advanced structural requirements as well as reduce maintenance concerns. These advanced materials provide many advantages over traditional structural materials, including high stiffness/strength to weight ratios, superior resistance to corrosion, reduced maintenance costs, and near net geometry part manufacturing capabilities. Correspondingly, there are also considerations that must be taken into account when considering the use of such materials, including reduced impact damage tolerances, jointed connections, and repair methods should damage be sustained. Furthermore, in certain applications there is an increased risk of severe loading and environmental conditions such as impacts, collisions, shock loading, and long term seawater exposure. While the static response of such materials is well understood, there is less of an understanding in terms of what happens to the same composite material when subjected to high loading rates. Therefore, there is a fundamental need to understand the behavior of these materials not only at static load levels but also at loading rates many orders of magnitude higher. Correspondingly, the ability to predict the load carrying capability of these materials after a damaging or shock loading event is critical to provide assurance that a component retains structural integrity and functionality. Furthermore, the degrading effects of long term environmental exposure on the mechanical properties of the materials should be quantified and understood in order to provide designs that will function

J. LeBlanc (✉) · E. Gauch
Naval Undersea Warfare Center, Division Newport, Newport, RI, USA
e-mail: James.M.LeBlanc@Navy.Mil; Erin.Gauch@Navy.Mil

C. Javier · A. Shukla
Department of Mechanical, Industrial and Systems Engineering, University of Rhode Island, Kingston, RI, USA
e-mail: Carlos_Javier@my.uri.edu; ShuklaA@uri.edu

S. W. Lee (ed.), *Advances in Thick Section Composite and Sandwich Structures*,
https://doi.org/10.1007/978-3-030-31065-3_2

throughout the expected service life of a specific structure. Due in large part to these uncertainties in the knowledge base related to these material systems there is a tendency to introduce large safety factors into structural designs which can have the effect of designing out the weight savings afforded by the materials.

When a submerged structure is exposed to an underwater explosion, it undergoes a complex and highly transient loading condition including high peak pressures and spherical wave fronts. When explosions occur at sufficiently large standoff distances from a structure, the shock fronts are nearly planar and act over the entire structure in a nearly uniform manner. This loading results in structural responses consisting primarily of flexure with large center-point deflections. However, there tends to be low levels of material damage (primarily inter-laminar delamination) and plate perforations or ruptures are minimal. In the absence of plate rupture, the shock wave is almost fully reflected away from the structure, shielding any occupants and/or internal equipment from the effects of the high pressure waves. Conversely, when an explosion occurs directly on, or very close to, the surface of a structure, the loading area is limited to the vicinity of the detonation itself. This loading is generally characterized by a spherical shock front impinging upon the structure as well as interaction of the UNDEX bubble and the target structure. The result is highly localized pressure loadings and significant damage, oftentimes including plate penetration or complete rupture. Upon rupture of the plate the pressure waves enter the structure, subsequently exposing any occupants to the adverse effects of high pressure gases as well as any shrapnel which may become dislodged from the blast area.

In recent years, there have been a multitude of research investigations which have studied the response of composite materials when subjected to highly transient and severe loading conditions. These investigations have explored the effects of blast and shock conditions through the use of a variety of advanced experimental techniques including the direct use of explosive charges, shock tubes, and underwater shock simulators. The work has also focused on a diverse range of structural configurations of interest ranging from flat solid laminates, to curved panels, cylinders, and sandwich constructions. Nurick et al. [1, 2] have studied the effects of boundary conditions on plates subjected to air blast loading and identified distinct failure modes depending on the magnitude of the impulse and standoff. Tekalur et al. [3] investigated the effects of shock loading on both E-Glass and Carbon based laminates. Mouritz [4] studied the effectiveness of adding a light weight, through thickness stitching material to increase the damage resistance of composites. The same author has also studied the effect of shock loading on the flexural [5] and fatigue [6] properties of composite laminates when subjected to underwater shock loading. These studies have shown that under relatively low impulsive loading the material sustains little damage (primarily matrix cracking) and the mechanical properties remain the same as for undamaged laminates. However, once a critical loading threshold is exceeded then the panels experience fiber breakage and the material strengths are significantly degraded. Dear and Brown [7] have conducted a detailed study on the damage mechanisms and energy absorption in composite plates when subjected to impact loading. Franz et al. [8] and LeBlanc et al. [9] have studied

the effects of shock loading on three-dimensional woven composite materials. Studies on the response of composites subjected to UNDEX have generally focused on far field loading in which the encroaching shock front is nearly planar and there is no interaction between the UNDEX bubble and the structure. LeBlanc and Shukla [10, 11] have studied the response of both flat and curved E-glass/epoxy composite plates to far field loading. Mouritz [4], conducted a study of the development of damage in a glass reinforced composite subjected to underwater explosive loading at increasing pressures. Both air backed and water backed conditions were evaluated. In the case of the water backed laminates no damage or degradation in strength was noted. In the air backed laminates delamination and matrix cracking led to a degradation of the residual strength of the composite. Recently, there has been an increased interest in the study of the effect of shock loading on sandwich structures. These studies include the effects of shock and impact loading conditions (Jackson et al. [12], Schubel et al. [13], Arora et al. [14]). Avachat and Zhou [15] studied the effects of underwater shock loading on filament wound and sandwich composite cylinder and found that while both constructions exhibited similar damage mechanisms, including delamination, fiber failure and matrix cracking, the sandwich structure had overall better performance than a monolithic cylinder with similar mass. The same authors [16] also utilized an Underwater Shock Loading Simulator combined with digital image correlation to show that for sandwich constructions lower density cores yield higher blast performance than high density cores due to their larger core compression capability. Work by Latourte et al. [17] utilized a scaled fluid structure method [18] to study the failure modes and damage mechanisms in both monolithic and sandwich plates subjected to underwater impulsive loads.

Analytical damage models for composites have been widely developed and are continually being refined and updated. These models typically assign an internal damage variable to each of the types of damage of interest (ie. matrix cracking, fiber rupture) which, in simple form, are ratios of the stress state to a failure criteria (Matzenmiller et al. [19], Zako et al. [20], Dyka et al. [21]). Based upon the expression representing each damage variable, the effective elastic properties can be degraded when the variable reaches a critical value. As the mechanical properties must be continually updated to account for the damage degradation this methodology lends itself well to implementation in finite element codes. The finite element modeling of damage in composites has been performed primarily on models simulating strain rates up to those representing drop test experiments with some work performed at the high strain rate regimes expected in shock loading. Material models are continually being implemented and refined in existing commercial finite element codes (O'Daniel et al. [22], McGregor et al. [23]). Recent publications involving computational modeling of damage progression in composites have utilized Ls-Dyna and the Mat_162 (Mat_Composite_OPTION) material model which simulates fiber breakage, matrix cracking and delamination damage. This material model combines the progressive failure theory of Hashin and the damage mechanics approach of Matzenmiller et al. [19]. Gama et al. [24] have published results from quasi-static punch shear loading experiments which correlate well with simulations

utilizing the Mat_162 material model. Simulations of low velocity impact experiments have been documented in the work by Donadon et al. [25], Hosseinzadeh et al. [26], and Tagarielli et al. [27]. Furthermore, Batra and Hassan [28] studied the response of composites to UNDEX loading through numerical simulations; however, there are no comparisons to experimental results. LeBlanc et al. [10] have presented a modeling methodology which simulates composite plates subjected to underwater explosive loading with comparisons to both the transient strain response as well as post mortem damage.

During the service life of marine structures there is typically an extended/prolonged exposure to the wetted environment, specifically aggressive salt water. As a result there is an ongoing body of research into the adverse effects of these conditions on component materials to the continuous exposure [29]. Additionally, these structures may be deployed into operations settings in which impact and shock loading is a concern. With these loading conditions in mind, failure to consider degradation of mechanical properties could be catastrophic. A significant cause of mechanical degradation in composites in a marine environment is the diffusion of water into the matrix material [29]. The diffusion process is relatively well established and can be described by a diffusion coefficient that is a function of parameters such as temperature, type of resin and curing agent, surrounding medium composition, fillers, void content, and so on. The value for diffusion coefficient and the theoretical models used to describe the diffusion varies in previous studies of diffusion in composites [30–37]. A standard and well-accepted model for epoxy resins, in terms of mass diffusions, is a Fickian model which uses Fick's second law to predict how the concentration of a diffusive substance changes over time within a material [38, 39]. Previous works used the Fickian model to study the properties changes during low strain rate loading of diffused composites. Current research on the high strain rate response of weathered composites is limited. Recently, there has been a study that analyzes the shock response of weathered composites plates within an air medium [40].

2 Far Field UNDEX Loading of Curved Plates

Two primary, underwater applications of composite materials are vehicle hull forms (ROV's, UUV's) and underwater pipelines. These uses generally result in curved structural geometries in which the curvature is oriented into the fluid domain (convex as viewed from the wetted surface). Thus there is an ongoing need to understand the complex loading, both temporally and spatially, that results when a highly transient shock pressure load is applied to a curved plate geometry. The transient structural response of the plates themselves is also of key interest. To this end, a detailed experimental and numerical investigation of the response of curved plates when subjected to far field shock loading was conducted. The far field pressure loading is characterized by a shock wave front that is nearly planar upon arrival at the structure of interest (i.e. shallow curvature with respect to the structural

geometry of interest). The primary objective was to develop a controlled experimental approach to subject curved composite plates to far field underwater explosive loading while capturing the transient response, along with development of a computational modeling method to accurately simulate the experiments.

2.1 Conical Shock Tube Facility and Experimental Method

A conical shock tube (CST) facility was utilized to impart shock loading to the composite plates in the study. The shock tube provides an effective and repeatable means for the conduct of underwater explosive testing representative of a far field detonation, generally characterized by planar, or very shallow wave front curvature. The shock tube is a horizontally mounted, water filled tube with a conical internal shape as illustrated in Fig. 1. The geometry of the tube itself is intended to represent an angular segment of the pressure field that results from the detonation of an explosive charge in a free field underwater environment; generally, a spherically spreading wave front. In the CST, the rigid tube walls confine the expansion of the pressure wave in a manner that simulates a conical sector of the pressure field. An amplification factor which relates the amount of explosive charge used in the CST to an equivalent spherical charge in a free field is defined by Poche and Zalesak

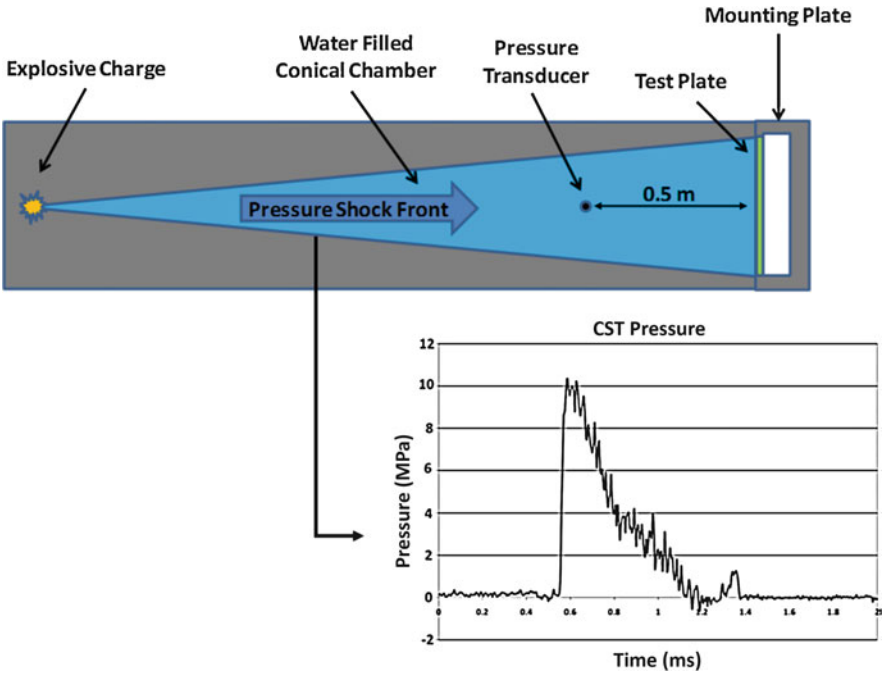

Fig. 1 Conical shock tube schematic (not to scale)

[41]. This is taken to be the ratio between the weight of a spherical charge, W, required to produce the same peak pressure at a given standoff distance as that produced in the shock tube by a segment of charge weight, w. Further discussion on the development and history of the water filled conical shock tube is provided by [42, 43]. The tube utilized in the current study has an internal cone angle of 2.6 degrees, is 5.25 m (207 in.) in length, and when flooded contains 98.4 L (26 gal.) of water at atmospheric pressure. The pressure shock wave is initiated by the detonation of an explosive charge at the breech end of the tube. A typical pressure profile obtained from the use of the tube is shown in Fig. 1 and is highlighted by the rapid rise time of the pressure followed by the exponential decay of the wave. The length of the tube is sufficient so that plane wave conditions are nearly established at the test specimen.

During testing, a mounting fixture which holds the composite plates with fixed edges and allows for air backing, was utilized as shown in Fig. 1. The plates are mounted with the convex face oriented towards the incoming shock front so as to represent a submerged underwater structure. The study has employed the use of high speed photography coupled with digital image correlation to capture the transient response of the plates during loading and subsequent deformation in real time. The advantage of such a non-contact, optical method in the experiments is full-field measurement as well as the elimination of strain gages and their inherent practice of debonding from the specimens at high shock levels and large plate flexures. The use of two cameras in a stereo configuration allowed for the three-dimensional, out of plane response to be captured. A framing rate of 20,000 frames/second was used with an inter-frame time of 50 μs. The explosive charge used in the study is an M6 blasting cap which yields peak pressures of 10.3 MPa at the pressure sensor location, .508 m (1.67 ft).

2.2 *Materials and Plate Geometry*

The composite plates utilized in the study are comprised of a 0°–90°, balanced construction biaxial, E-Glass / Vinyl laminate. The fabric consists of 0/90 layers that are stitched (non-woven) and have a dry areal weight of 0.406 kg/m^2. Each plate has a finished part thickness of 1.37 mm (0.054 in.), a fiber content of 62% by weight, has 3 plies of the fabric, and has mechanical properties provided in Table 1. The plates contain a curved midsection with the convex face having a radius of curvature

Table 1 E-Glass /Vinyl ester biaxial laminate -mechanical properties (ASTM 638)

	MPa (lb/in^2)
Tensile modulus (0°)	15.8e3 (2.3e6)
Tensile modulus (90°)	15.8e3 (2.3e6)
Tensile strength (0°)	324 (47,000)
Tensile strength (90°)	324 (47,000)

of 18.28 cm (7.2 in.) and an outer diameter of 26.54 cm (10.45 in.) with a 22.86 cm (9 in.) unsupported middle section.

2.3 Computational (Finite Element) Model Overview

The conical shock tube experiments have been simulated through the use of the LS-DYNA finite element code. The objective of the numerical modeling is to demonstrate an approach which is able to capture both the complex fluid structure interaction that occurs between the shock front and the curved plate surface as well as the transient deformation mechanisms that the plate undergoes as a result of the loading. The complete finite element model of the CST test setup utilized in the study is shown in Fig. 2. The model consists of the internal fluid contained within the shock tube itself as well as the composite plate. The fluid within the tube is considered in the simulation so as to accurately represent the fluid structure interaction (FSI) at the interface of the fluid and test plate. The simulations show that during the interaction of the pressure wave and the curved surface of the plate the pressure loading on the plate is not uniform across its face. Thus the inclusion of the fluid is a critical aspect of the modeling approach. In the model, the pressure profile that is

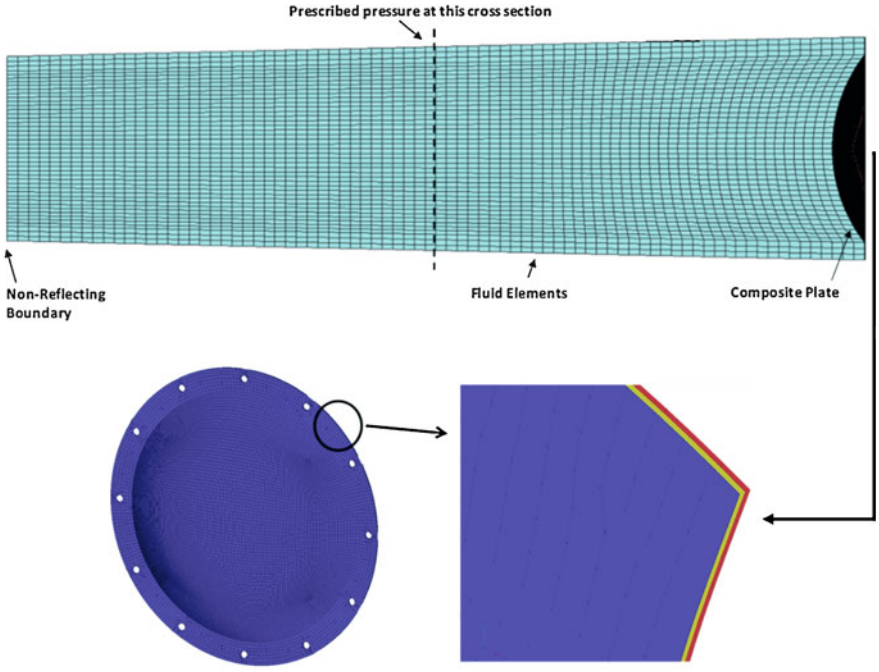

Fig. 2 CST and Composite plate model

recorded by the pressure sensor is mapped into the fluid domain at a tube cross section corresponding to the sensor location and the wave is propagated numerically from that point towards the plate surface. The fluid is modeled with solid elements and a null material definition which allows for the material to be defined with an equation of state (EOS). The linear polynomial EOS is utilized in the models and allows for the bulk modulus and density of the water to be defined. This allows for an accurate propagation of the pressure wave in the water in a computationally efficient manner. Fluid–structure interaction between the water and the composite plate is numerically coupled through the use of a tied-surface-to-surface contact definition.

The composite plate in the simulations is modeled using shell elements with the plate model consisting of 3 layers of shell elements, each layer representing a 0° and 90° combined ply, Fig. 2. The mid-surface of each ply is meshed and the individual shell layers are offset by the ply thickness. The material model utilized in this work is Mat_Composite_Failure_*Option*_Model which is an orthotropic material definition capable of modeling the progressive failure of the material due to any of several failure criterion including tension / compression in the longitudinal and transverse directions, compression in the through thickness direction, and through thickness shear. It is important to note that failure in one direction does not cause the element to be deleted. An element is only deleted from the analysis after it has failed in all directions and can no longer carry any load. Delamination damage is considered and is taken into account through the use of a surface-to-surface tiebreak contact definition. The tie break definition initially ties the nodes between plies together to inhibit sliding motion. The force at each node is monitored by the software and the corresponding normal and shear stresses are computed. If the current stress state at any node in the contact definition exceeds the failure criteria then the tie definition for that node is deleted and the node is free to slide, thus individual plies can separate but not pass thorough one another.

2.4 Simulation Results and Correlation to Experiments

The complex fluid structure interaction between the incident shock front and the curved composite plates was visualized through the use of the computational models. Due to the solid walls of the CST only the pointwise pressure history at the pressure sensor was obtained during the experiments. The pressure wave propagation and corresponding interaction with the curved surface of the plate is detailed in Fig. 3. Correspondingly, the transient plate response is shown in the right side of Fig. 3. The results presented identify several significant observations. The first is that while the pressure wave in the tube is nearly planar during its propagation towards the panel, upon its interaction with the curved surface the pressure loading becomes complex and not uniform. Noticeably, there is a low pressure area that develops in the center of the plate while the clamped edge sustains a higher pressure magnitude. Due to the air-backed nature of the plates and the relative thinness, the middle of the plate has a low stiffness as compared to the clamped edge of the plate. A second key

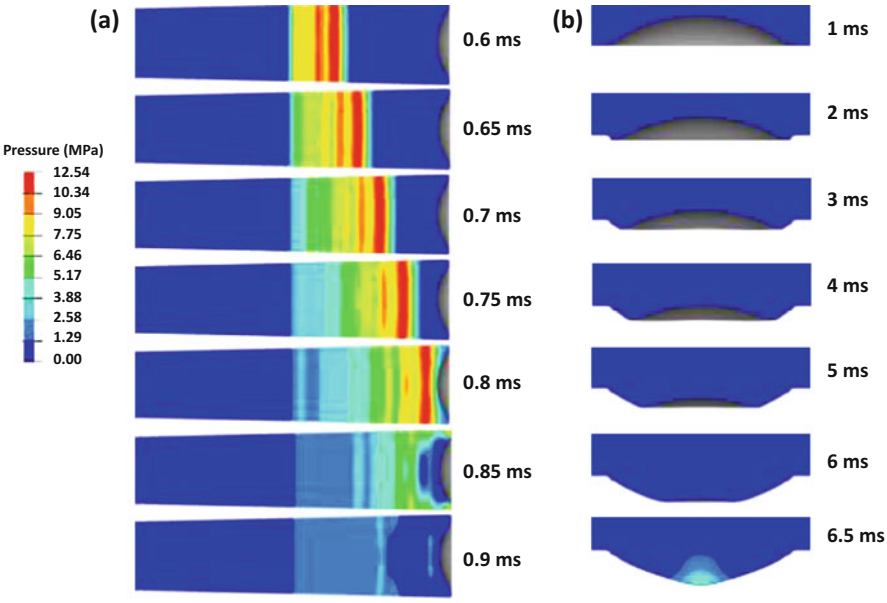

Fig. 3 (**a**) Fluid structure interaction, (**b**) Plate deformation progression

observation is that there are two distinct time regimes in the problem of interest as it relates to the plate mechanics. The first is a very short duration of time, 0.2 ms, in which the pressure wave loads the plate surface followed by a longer period of time, ~5 ms, in which the plate undergoes the physical deformation. The mechanics of the plate deformation consist of a full inversion process, with three key mechanisms. Initially, a hinge forms at the outer edge of the plate at the clamped boundary, which subsequently propagates towards the center of the plate, and finally is arrested upon reaching full plate inversion at 6.5 ms. Corresponding to the arrest of the inversion process there is a high pressure region that develops at the apex of the inverted shape caused by the fluid that was following the plate surface coming to a sudden stop.

The displacement and velocity data that was captured during the experiments is used to demonstrate correlation between the results and the simulation data. The back face, transient data as recorded through DIC is the primary means for correlation, namely the center-point time history displacement and the corresponding full field deformation profiles. The agreement between the simulation and experiment time histories is shown in Fig. 4 and the full field correspondence is highlighted in Fig. 5. The center-point displacement comparison shows that the experiment and simulation results agree nearly exactly early in the event and then the displacement in the experiment occurs slightly faster than the simulation. The full field comparison of the deformation evolution exhibits good correlation in terms of the displacement evolution and the full inversion of the panels as a result of the shock pressure loading. There is some level of non-symmetric behavior observed in the experimental results whereas in the simulations the deformation is symmetric as expected. In

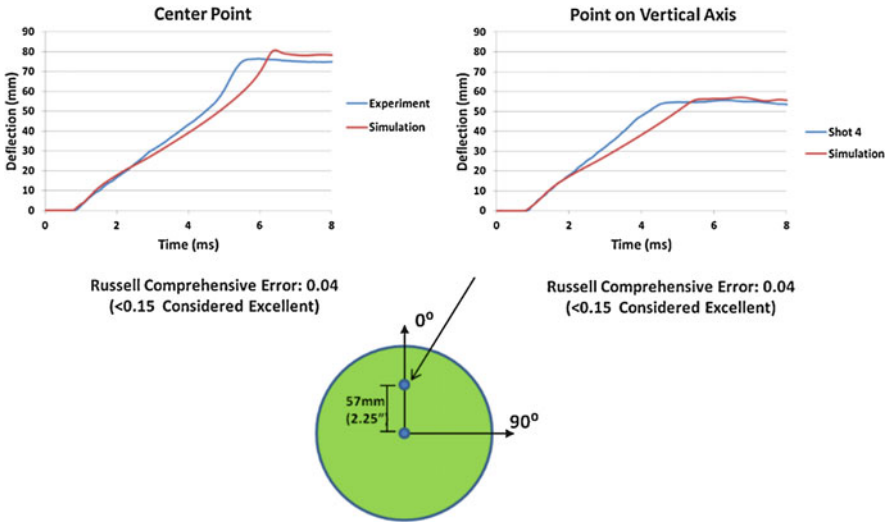

Fig. 4 Time history deformation comparison of experiment and simulation

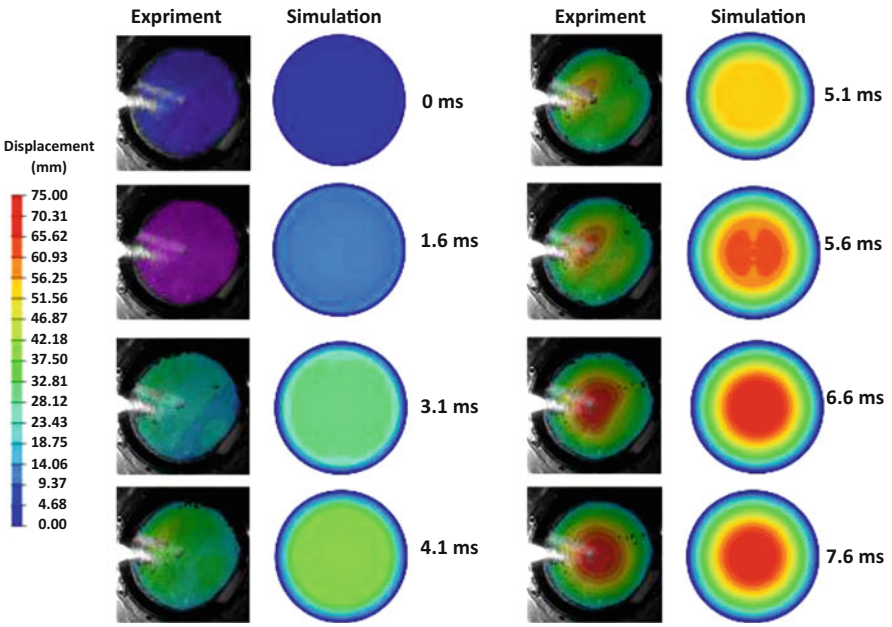

Fig. 5 Full field deformation comparison of experiment and simulation

addition to the transient correlations, the relationship between the material damage observed during the test and the damage level predicted by the simulations is correlated. In the experiment the main damage mechanism that was observed is delamination between the plies with minimal fiber rupture or matrix cracking. The

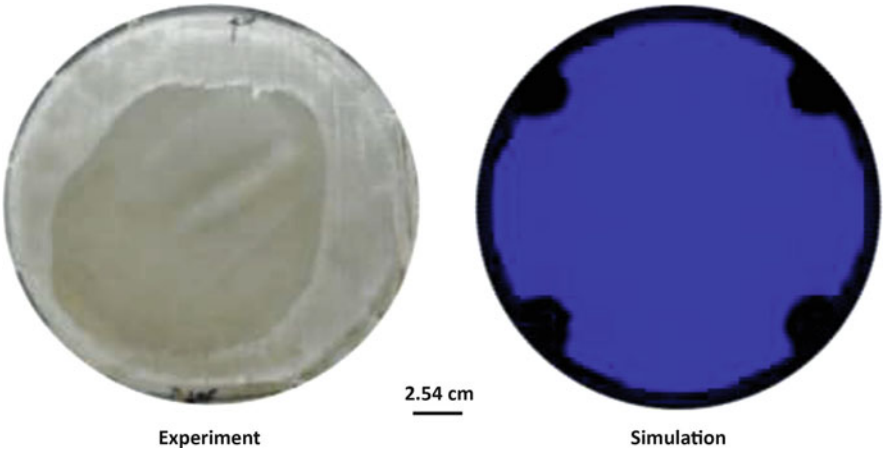

Fig. 6 (**a**) Material damage during test, (**b**) Material damage from simulation

final damage state from the shock test and corresponding simulation is shown in Fig. 6 where in the experimental image the damage is indicated by the lighter material and in the simulation the delamination area is highlighted by the black area. Although the amount of delamination is somewhat larger in the experiment than is observed in the computational model, it is encouraging that the model is able to predict the onset of the delamination itself and propagate it to a comparable distance. In the models the delamination criterion was taken to be 36 MPa (5250lb/in^2) for both tensile and shear stresses which corresponds to approximately one-half of the tensile strength of the pure vinyl ester. The degradation by ½ of the tensile strength accounts for voids, and interfacial defects / flaws between the layers of fibers during the manufacturing of the material. This observation is provided to aid in the development of delamination modeling best practices but is not meant to be definitive, rather further work in this area is required.

2.5 Key Findings

The investigation described in this section has studied the response of curved composite panels to far field underwater explosive loading conditions through both novel experiments and advanced computational models. The experiments were performed through the use of a conical shock tube facility which provides a controlled and repeatable means for the conduct of underwater shock testing representative of much larger charges in a laboratory setting. The use of computational models to supplement the experimental work allows for additional insight into the physics of the experiments which would otherwise be difficult to ascertain, namely the fluid structure interaction between the pressure wave and the plate surface. The specific material evaluated in the study is an E-Glass / Vinyl Ester bi-axial laminate

with fibers balanced in the 0 and 90 degree directions. The plates are convex in geometry and oriented with the curved face towards the incident shock front. The correlation between the experimental and simulation results demonstrated high agreement at both the pointwise and full field deformation levels. Furthermore, the simulations were able to highlight that the loading of the plates by the pressure and the resulting deformation evolution could be separated into two distinct time regimes, with the pressure loading occurring over a fraction of a millisecond and the deformation occurring over several ms. The significant finding of the work is that computational tools can serve to support experimental test results and show promise for use as an alternative to testing to support structural designs utilizing composite materials.

3 Near Field UNDEX Flat Plates

Subsequent to the far field UNDEX experiments which were described in the preceding section, an experimental and numerical study was undertaken to investigate the response of flat composite plates when subjected to near field loading conditions. The near field blast loading condition is encountered when an explosion occurs directly on, or very close to, the surface of a structure. The result is highly localized pressure loadings and the structure sustains higher amounts of damage, oftentimes including plate penetration or complete rupture. The work presented in the following section discusses the effects of the near field blast loading on not only baseline composite plates, but also investigates the effects of structural plate thickness and the application of polyurea coatings on both the transient response as well as damage levels sustained in the material. The investigation consisted of experiments performed in an underwater blast tank including the use of Digital Image Correlation (DIC) to capture the transient response of the plates along with corresponding computational simulations performed with the commercial finite element code LS-DYNA.

3.1 Materials and Plate Configurations

The composite material utilized in the study consists of a commercially available, bi-axial E-Glass/Epoxy laminate, specifically Cyply® 1002. The panels are of non-woven construction with continuous, parallel fiber orientations. The cross ply construction has alternating 0 and 90° plies of which each is 0.254 mm thick. The laminates have an areal weight of 0.46 kg/m^2 (0.85 lb./yd^2) per ply and a resin content of ~36%. To determine the relative influence of panel thickness on the transient and damage performance of the plates, two thicknesses are considered, 0.762 mm and 1.524 mm. Furthermore, for the 0.762 mm plates a polyurea coating of thickness 0.762 mm has been applied to the back surface of the plates, resulting in

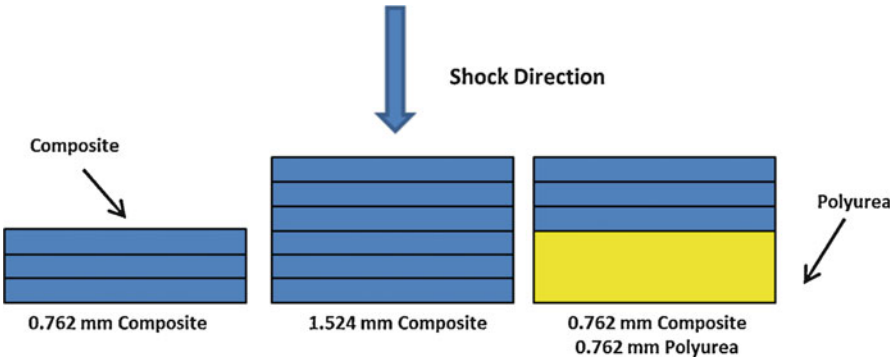

Fig. 7 Composite plate construction – Schematic (Not to scale)

an overall coated plate thickness of 1.524 mm. The plate configurations that have been studied are: (1) 0.762 mm thick uncoated plate, (2) 1.524 mm thick uncoated plate, and (3) 0.762 mm thick plate with a 0.762 mm polyurea coating on the back face. The schematic of the panel configurations investigated are provided in Fig. 7. The polyurea was sprayed onto the plates and then post cured for 48 h at a temperature of 160 °F. The specific polyurea material used is Dragonshield-BC and is a 2 part, spray cast material. Mechanical characterization of the coatings was performed in both tension and compression from strain rates from 0.01 s^{-1} to 2000 s^{-1}. Characterization up to 100 s^{-1} was performed using standard material testing machine whereas a split Hopkinson pressure bar was used to characterize the response of the material at 2000 s^{-1}. The full material characterization including loading direction and strain rate dependence is shown in Fig. 8. Moreover, the material exhibits strong strain rate dependence and becomes stiffer with increasing loading rate.

3.2 UNDEX Facility and Experimental Method

One of the primary focuses of the current study is the implementation of an experimental approach for the subject of flat plates to near field UNDEX conditions in a controlled laboratory environment. The conduct of such testing allows for highly controlled and repeatable experiments to be performed while also employing measurement techniques that would be difficult to utilize in a larger scale or operation test theatre. To that end, the study described in this section makes use of a water filled blast tank coupled with high speed photography and Digital Image Correlation to impart UNDEX loading to the fully clamped plates while capturing the full-field transient response. The experiments in this study were conducted in a water filled tank with internal dimensions of 1.21 m × 1.21 m × 1.21 m (3.94 ft. × 3.94 ft. × 3.94 ft) as shown in Fig. 9. Four window ports allow for the lighting and high speed photography of the UNDEX event and plate motion. Mounted to the inner surface of

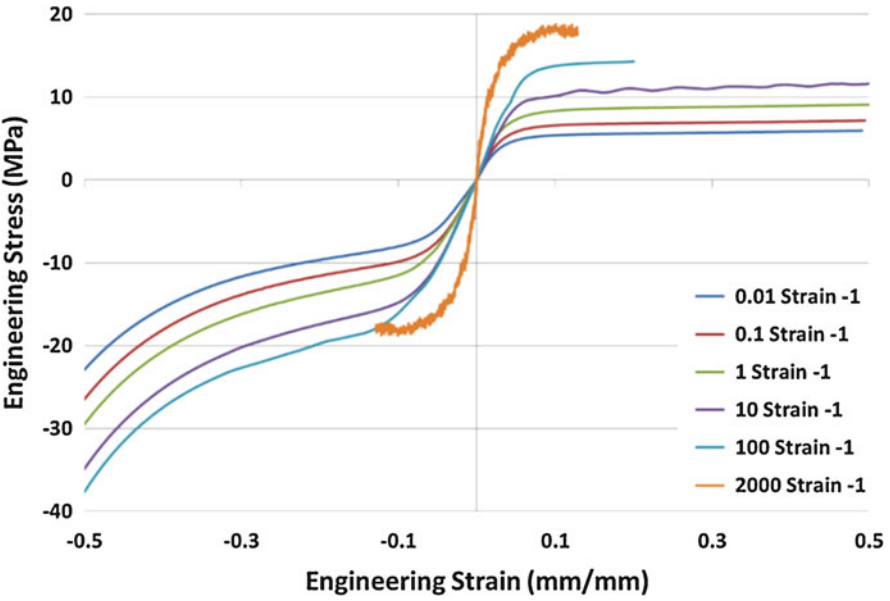

Fig. 8 Dragon shield BC polyurea stress-strain behavior

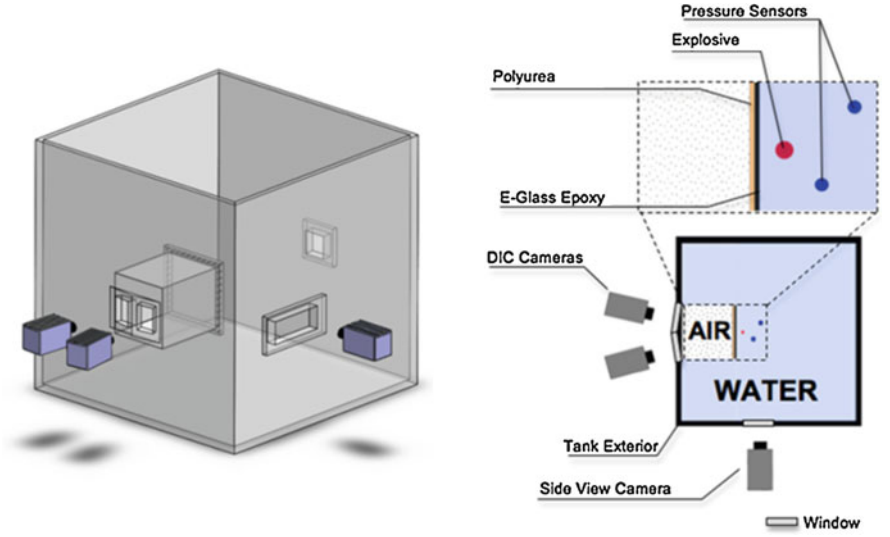

Fig. 9 UNDEX test tank

one wall is a 304.8 mm × 304.8 mm (1.0 ft. × 1.0 ft), rectangular tunnel with a wall thickness of 12.7 mm (0.5in), which serves as the base for the mounting of the composite plates. The use of the tunnel and a water tight mounting fixture allow for the plates to be air backed. The explosive used in the near field blast experiments is

an RP-503 charge manufactured by Teledyne RISI. The charge is comprised of 454 mg RDX and 167 mg PETN contained within an outer plastic sleeve. It is suspended by its detonation wire into the tank and placed 50.8 mm (2.0in) from the center of the composite plate. To ensure consistent charge standoff distances for each experiment a 3.18 mm (0.125in) diameter foam spacer is placed between the charge and plate. The foam is secured to both the charge and plate by a fast setting epoxy. Free field dynamic pressure transducers located within the fluid field capture the pressure wave which results from the explosive detonation. High speed photography, coupled with three dimensional Digital Image Correlation (DIC) was used to capture the full-field deformation of the back-face (side opposite of the explosive) of the plates during the UNDEX loading. Two high speed cameras were positioned 330 mm (12.9in) behind the tank walls perpendicular to the viewing windows to avoid any distortion effects from the windows themselves. A third high speed camera was positioned at the side of the tank to view the detonation of the explosive, resulting bubble growth, and interaction of the bubble with the composite plate. The cameras used during experimentation were Photron FastCam SA1 and a frame rate of 27,000 fps was utilized for an inter-frame time of 37 μs.

3.3 *Computational Model*

A fully coupled fluid-structure interaction modeling approach for the simulation of the near field explosive experiments was developed through the use of the commercial LS-DYNA code. Specifically, the Lagrange-Eulerian formulation of the code has been adopted in the investigation as it allows for accurate representation of the detonation of the explosive charge as well as the fluid structure interaction between the fluid and the composite plate. A schematic of the full simulation model is shown in Fig. 10, and is seen to consist of the composite plates (uncoated and coated), the

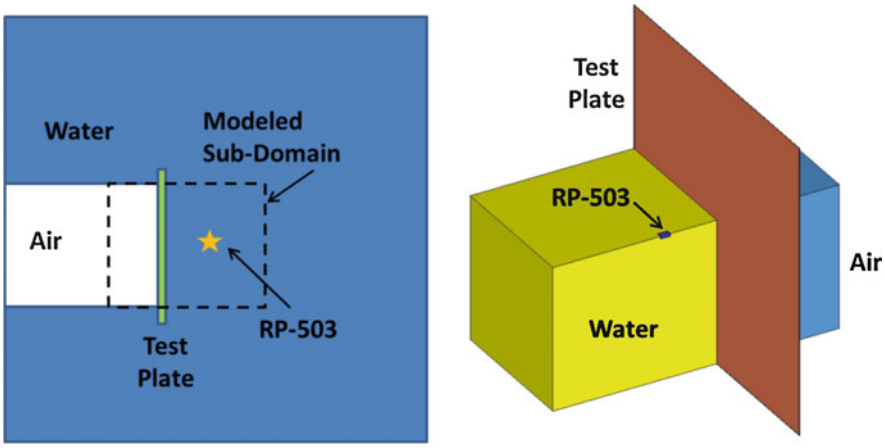

Fig. 10 Finite element model of UNDEX experiment (3 Quadrants of fluid domain hidden)

water within the tank, the air behind the plates and, the RP-503 charge. For efficiency only a subdomain of the full tank facility is explicitly modeled in the simulations consisting of the unsupported section of the composite plate, 120 mm (4.72in) of air extending behind the plate, and 200 mm (7.87in) of water extending from the plate surface towards the charge. This subdomain approach is deemed appropriate as the loading of the plate and subsequent response occurs sufficiently fast that reflections from the tank walls do not affect the overall transient response of the plate. Furthermore, the outer surface of the fluid sub-domain is prescribed a non-reflecting boundary condition which allows the associated pressure waves to freely leave the domain rather than reflect off of the free numerical surface. In the model the water, air, and explosive charge are modeled using an ALE multi-material element formulation and is fully described through the use of a material definition in combination with an equation of state (EOS). The water and air utilize the ∗Mat_Null material definition with the density of the water and air given as 1 g/cm^3 and 0.0013 g/cm^3 respectively. The Gruneisen EOS is used for the definition of the water with the speed of sound taken to be 149,000 cm/s. A Linear Polynomial EOS describes the air domain in the model by defining C_0, C_1, C_2, C_3, and C_6 equal to zero, and C_4, and C_5 equal to γ-1. The RP-503 charge is modeled with the ∗Mat_High_Explosive_Burn material model combined with the JWL EOS. The structural components of the model, namely the composite plate and polyurea coating, are represented by shell and solid elements, respectively. The plate in the simulations is modeled using a single layer of shell elements with the laminate schedule prescribed in the shell section definition including the angle of each respective ply and the orthotropic properties of each layer. The composite mechanical properties are defined through an orthotropic material definition (Mat_Composite_Damage) capable of modeling the progressive failure of the material due to any of several failure criterions including in-plane shear, tension in the longitudinal/transverse directions, and compression transverse direction. The polyurea material is modeled as solid elements and are assumed to be perfectly bonded to the composite plate. The material model for the polyurea coating is a viscoelastic material definition which captures both the strain and strain-rate effects through the use of a family of load curves. The model reproduces the uniaxial tension and compression behavior as obtained through material testing at discreet strain rates.

3.4 Experimental and Numerical Results

The response of the composite plates in this study is characterized by the transient center-point displacement of the back-face of the plate, deformation evolution mechanisms during the displacement, and full-field DIC observations.

The pressure profiles resulting from the detonation of the RP-503 charge, as measured by the two free field pressure sensors at 100 mm (3.93in) and 175 mm (2.95in) standoff distances from the charge, are shown in Fig. 11. The pressure

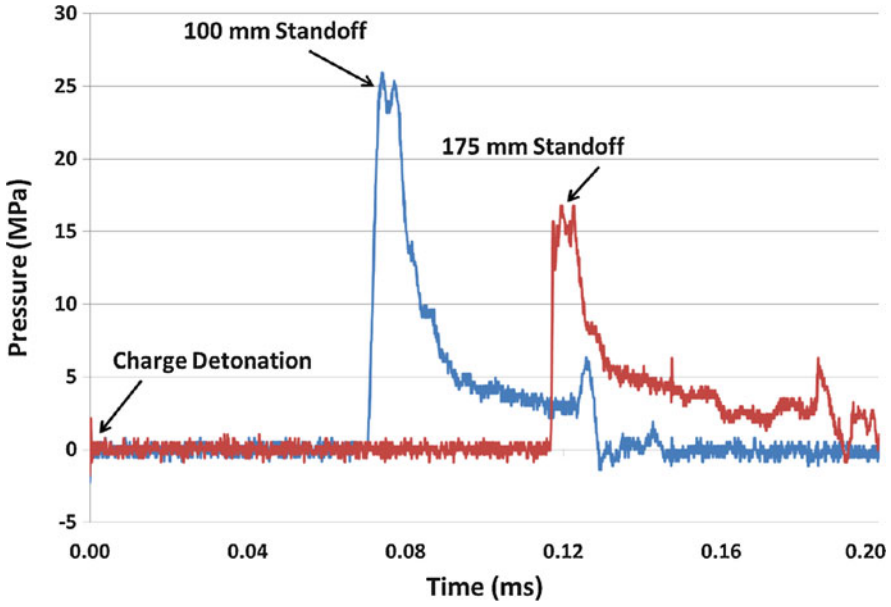

Fig. 11 UNDEX pressure profiles (Time zero corresponds to charge detonation)

profiles display the characteristic components of an UNDEX, namely: a rapid pressure increase associated with the shock front, followed by an exponential decay and a reduction in peak pressure with increasing radial standoff from the charge center. The behavior of the bubble resulting from the detonation and its associated interaction with the composite plate is shown in Fig. 12. The sequence of images shows the clear formation of the bubble at 80 μs and its subsequent growth in size due to the combustion of the explosive products. Due to the high pressure of these gaseous products the bubble expands, reaching a diameter of ~50 mm (1.97in) at 320 μs at which point it reaches and interacts with the surface of the composite plate. As a result of this interaction with the plate it is prevented from further expansion in the direction of the plate but continues a spherical expansion in the remaining directions.

As a result of the initial pressure loading from the detonation of the charges the composite plates deform primarily in the form of outward flexure (towards the air backing). The DIC data is used to capture both the pointwise (center) as well as the full field deformation evolution. Center-point time histories for each of the respective plate configurations is provided in Fig. 13 from which several key observations are made. The first observation that can be made is drawn from the comparison of the overall peak displacements of the plate. It is evident that, as compared to the baseline 0.762 mm (.03in) plate, increasing the plate thickness or including a polyurea coating reduces the peak overall deflection for a given level of loading. The center-point deflection comparison between the 1.524 mm (0.06in) uncoated plate and the 0.762 mm (0.03in) plate with a 0.762 mm (0.03in) coating of polyurea

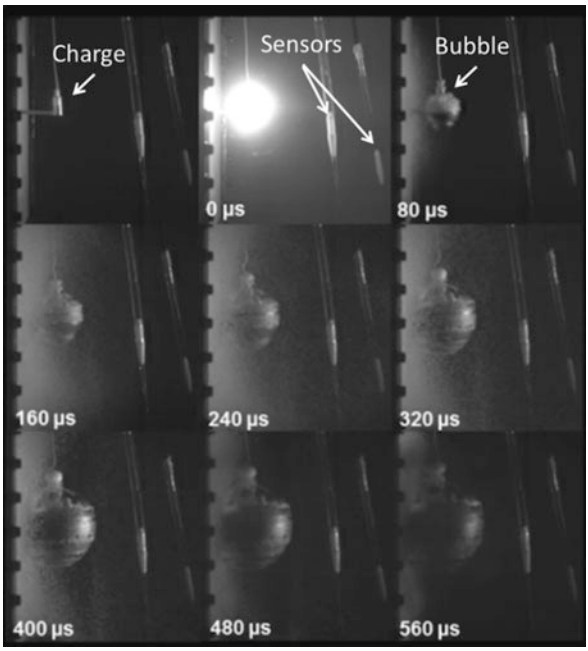

Fig. 12 UNDEX gas bubble behavior

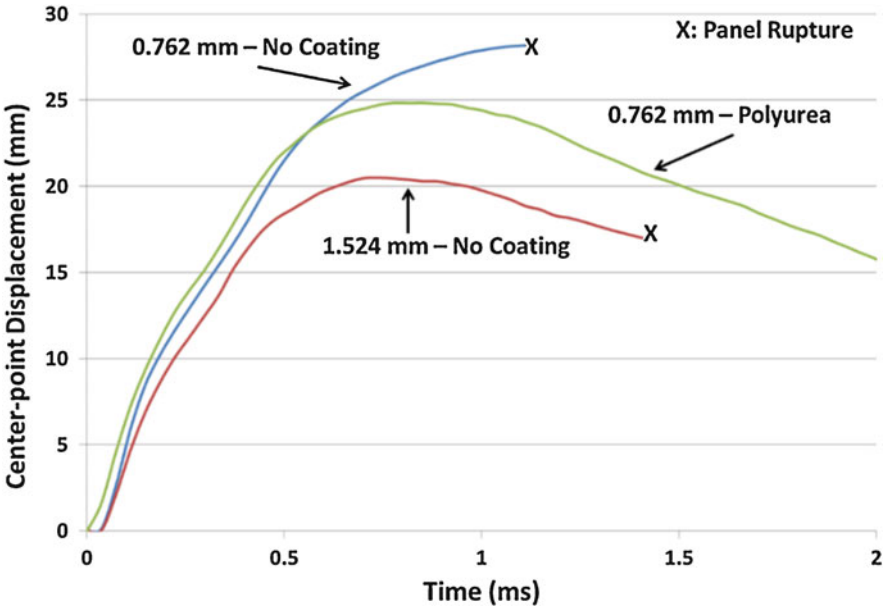

Fig. 13 Plate center-point deflections

indicate that for a given plate thickness it is more advantageous to utilize additional structural plies rather than an elastomeric coating. However, when a structure has previously been designed and further thickening of the structural shape is not possible, the application of a polyurea coating can improve the transient response to shock loading. The second primary observation from the time histories is related to the material damage initiation. Both the uncoated 0.762 mm (0.03in) and 1.524 mm (0.06in) specimens experienced significant through-thickness tearing at the plate boundaries at approximately 1.1 and 1.4 ms respectively. Furthermore, it is observed that although the 0.762 mm (0.03in) plate with the polyurea coating did experience larger deflections than the 1.524 mm (0.06in) uncoated plate, there was no edge tearing of the plate itself. Thus in terms of reducing material damage itself, the polyurea coatings offer an advantage over a thicker uncoated plate. The full field deformation evolution for each of the respective panels is shown in Fig. 14. The contours of out of plane displacement show that the deformation is initially dominated by localized deflections at the center with minimal deflection near the boundaries. As the plate responds to the pressure loading, it gradually transitions to an overall plate flexure mode as shown by the cross sectional shape at 0.74 and 1.11 ms. The significant observation is that the initial plate deformation is governed by the

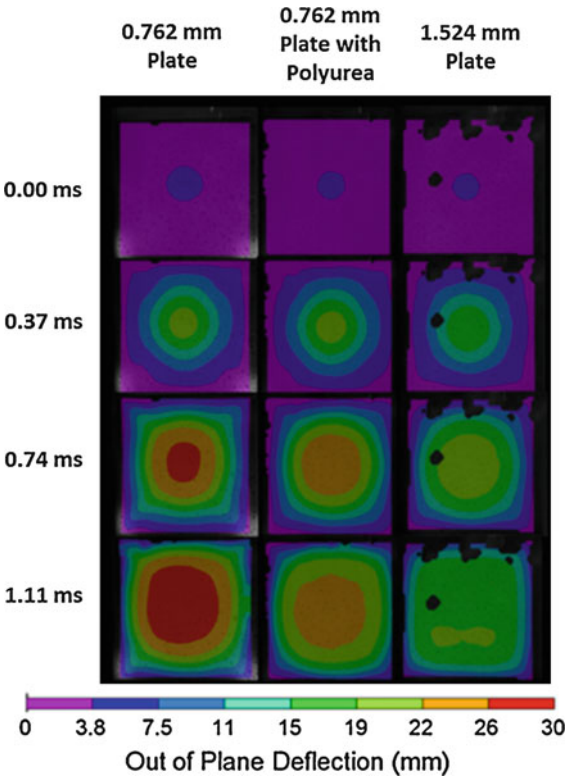

Fig. 14 Full-field deflection contours

highly localized pressure loading and then subsequently shifts to a mode I flexure deformation profile later in time.

The primary means for demonstrating the accuracy of the computational models in the investigation is through correlation of the center-point time histories and onset of material damage. The quality of the correlation between the test data and numerical results in this study is shown in the transient time histories shown in Fig. 15 for each of the panel configurations considered. Observation of the trends show that there is a high level of correlation between the experiment and simulations, both in terms of timing and overall peak deflections. The comparisons exhibit consistent results in the early time frame of the event (0–0.4 ms) in terms of displacement with minor discrepancy observed beyond this point. Furthermore, in terms of material damage onset, for both of the uncoated plate configurations (0.762 mm (0.03in) and 1.524 mm(0.06in)), it is seen that the onset of edge tearing occurs slightly later (0.1 ms) in time as compared to the experimental results. The timing differences in the onset of damage is expected as the model assumes a uniform plate in terms of material properties and does not account for manufacturing variability or minor internal defects which can contribute to the onset of damage or slightly weaker/stronger areas of the plates as compared to the gross material strengths.

3.5 Significant Findings

With the objective of investigating the characteristics of composite plates (including the effects of polyurea coatings) subjected to near field underwater explosions a detailed experimental and computational study was conducted. The primary focus of the work was on determining how the response of the plates was effected by increased plate thickness or through the application of a rate-sensitive, elastomeric coating to the baseline plate. The experiments were conducted in a water filled blast tank which allowed for laboratory scale, controlled testing to be completed while also allowing for the use of Digital Image Correlation to capture the full-field, transient response of the back (dry) surface of the plates. The experiments were complemented by corresponding fully coupled fluid structure interaction simulations. The response of three unique plate configurations was evaluated: (1) 0.762 mm (0.03in) baseline plate, (2) 1.524 mm (0.06in) plate, and (3) 0.762 mm (0.03in) plate with a 0.762 mm (0,03in) polyurea coating applied to the back-face. The significant findings of the study are:

1. The transient response of the plates is influenced by both overall plate thickness as well as the application of the polyurea coating. In terms of net effectiveness, the additional structural thickness reduced the transient deflections more than the inclusion of the coatings.

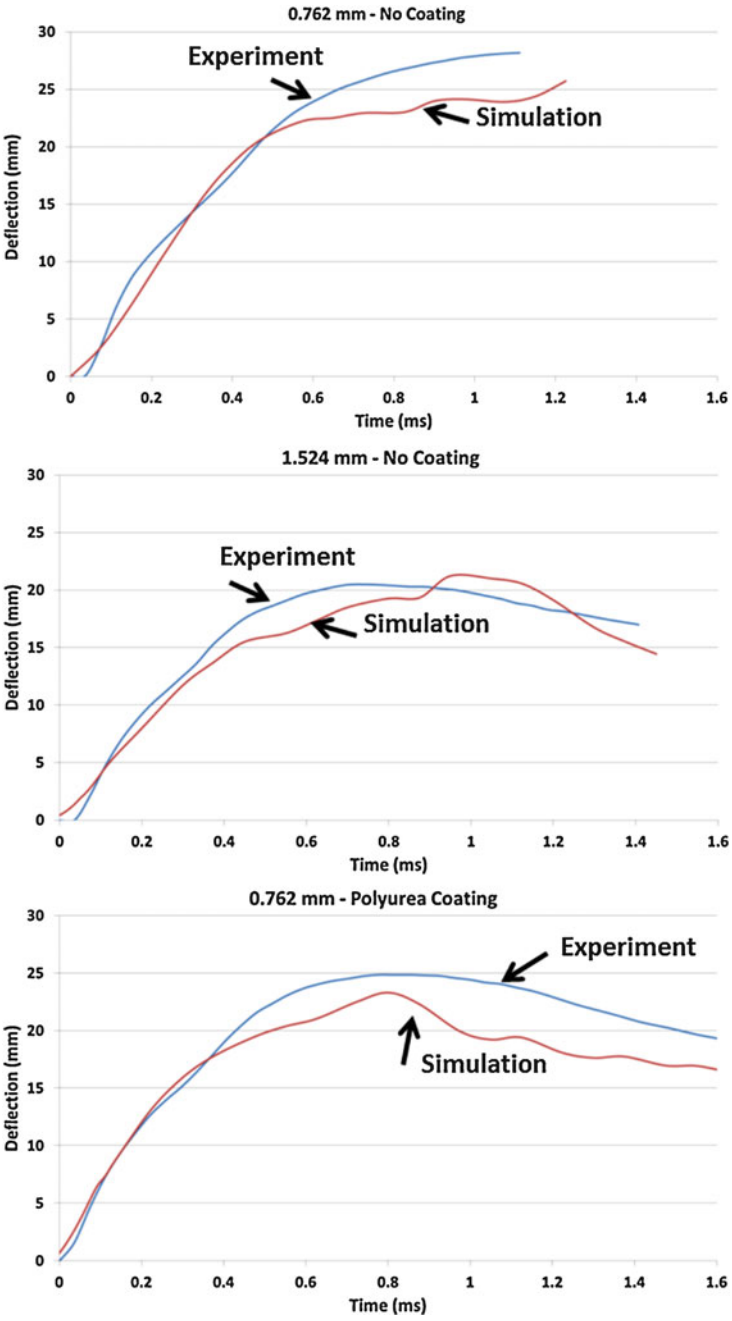

Fig. 15 Center-point displacement model correlation

2. As it relates to material damage sustained by the plates, the polyurea coating was more effective in reducing material damage as compared to both the baseline and thicker uncoated plates.
3. The computational modeling approach employed in the study is able to accurately capture the transient deformation of the plates undergoing shock loading as well as capture the onset of material damage consistent with the experimental results.
4. When considering a plate design, the desired performance metric of the plate response should be considered. A thicker plate of structural material (composite) is preferable to reduce center-point deflection, while the use of polyurea coating are effective in reducing overall damage. However, in the case of an existing design the use of polyurea coatings can be an effective retrofitting application to improve the blast resistance of a structure while reducing overall material damage.

4 Near Field UNDEX of Cylinders

Many undersea vehicles take the form of cylindrical, or cylindrically based, hull forms and therefore there exists a need to understand the physics of underwater blast waves with such geometric shapes. Thus, an experimental and computational study was conducted to investigate the transient response and material damage characteristics of composite cylinders when subjected to highly localized pressure loading conditions resulting from an underwater explosive (UNDEX) detonation. The key aspects of the study include evaluating the transient response of the cylinders due to the complex loading due to the detonation, the resulting material damage levels, as well as evaluating the effects of the elastomeric coatings in terms of damage reduction and energy levels.

4.1 Cylinder Specimens

The investigation included E-glass/epoxy, roll wrapped composite cylinders with a bi-axial laminate structure. The cylinders were tested in an uncoated base configuration as well as a configuration in which the polymeric coatings were applied to the outer surface in two thicknesses as shown in Fig. 16. The cylinders themselves have a wall thickness of 1.14 mm with 4 plies through the thickness and a laminate schedule of [0/45/45/0]. The laminates had a resin content of ~38% by weight and an areal weight of 0.49 kg/m2 per ply. The outside diameter of the cylinder is 7.44 cm with an unsupported length of 38.1 cm. The cylinder is fitted with an aluminum endcap protruding 12.7 mm into the length of the cylinder which seals against water intrusion via a rubber o-ring. Several cylinders were coated with polyurea, specifically Dragonshield-BC, through a spray-cast process to the outer surface. Thicknesses of 100% and 200% of the composite wall thickness were applied to evaluate

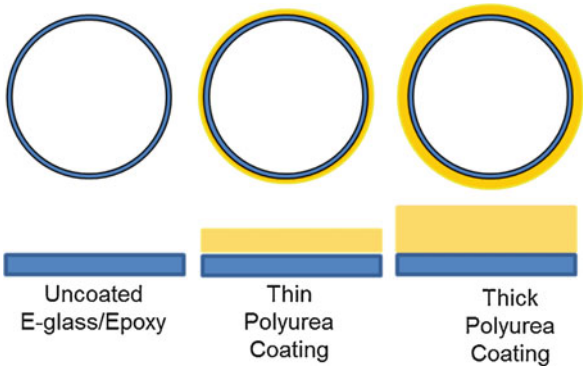

Fig. 16 Cylinder construction

the effect of the coating thickness parameter. This configuration is intended to be representative of a post-design (retrofit) coating application. The polyurea material properties are identical to those previously used during the flat plate experiments.

4.2 Experimental Method

The following is an overview of the experimental methodology that was employed in the study. A large diameter pressure vessel has been utilized for the conduct of all experiments in the study. The vessel has an internal diameter and height of 2.1 m with an array of windows along the horizontal axis of the test tank to allow for high speed photography to be conducted during the experiments. Each cylinder is mounted and held in the center of the tank with tensioned cables to minimize rigid body motion of the test article during transient loading. Dynamic pressure sensors located around the cylinders capture the pressure resulting from the explosive detonation as well as the subsequent bubble loading phases. Each cylinder configuration (base composite, thick coating, and thin coating) was tested at two charge stand-offs, 2.54 cm and 5.08 cm. All experiments were conducted at ambient pressure within the flooded tank. The test facility and experimental setup is detailed in Fig. 17. In each respective experiment, an RP-503 explosive charge containing 454 mg of RDX and 167 mg of PETN was utilized. Three high speed video cameras, FastCam SA1, were used to capture video during experiments with one camera mounted to align with the longitudinal axis of the cylinder, providing a side view of the UNDEX event and two cameras were arranged to provide a stereoscopic view of the cylinder on the opposite side of the explosive. Images were captured at a frame rate of 36,000 fps.

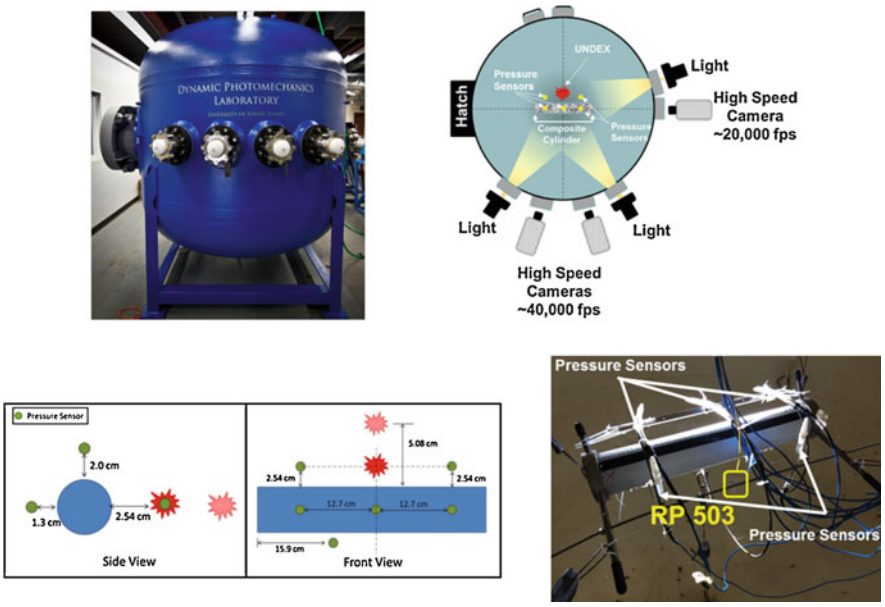

Fig. 17 Test configuration and sensor layout

4.3 Key Experimental Results and Findings

4.3.1 Bubble-Cylinder Interaction and Local Pressures

The near field nature of experiments resulted in a complex interaction between the UNDEX bubble and the cylinders, highlighted by a unique splitting of the bubble around the cylinder. Subsequent to the formation of the initial UNDEX bubble, a split occurred in which one portion of the bubble wrapped around onto the non-charge side with the bulk remaining on the charge side. As the initial pressure wave from the detonation passes over the cylinder, small cavitation bubbles form on the surface of the cylinder, which then subsequently coalesce and collapse against the surface after about 1 msec. Figure 18 provides images of key developments observed during the bubble-structure interaction during an experiment conducted at a charge standoff of 2.54 cm on a cylinder with a thick coating applied. No significant differences were noted in the bubble interaction between uncoated and coated cylinders. The large bubble which forms on the non-charge side of the cylinder, due to the splitting phenomenon, collapses upon itself at approximately 12.7 msec and serves to cause a secondary loading of the cylinder.

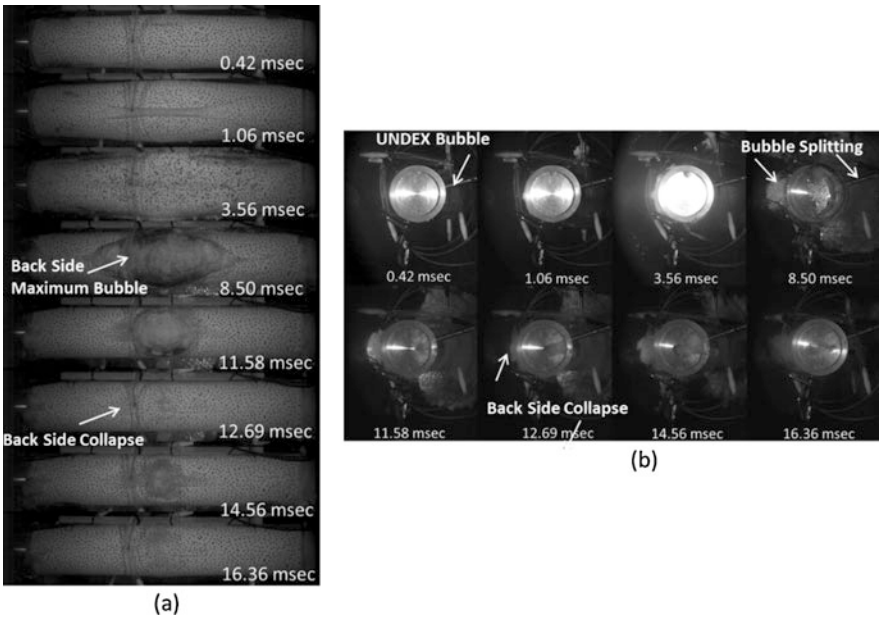

Fig. 18 Bubble growth and interaction (**a**) Front view, (**b**) Side view

4.3.2 Transient Cylinder Response

The physical response of the cylinders to the near field UNDEX loading is characterized primarily by flexure of the cylinder and quantified by the radial displacement of the center point on the non-charge side of each cylinder. Comparisons between the coated and uncoated specimens are limited to the time period for which DIC results are available due to cavitation effects which preclude DIC correlation later in time. The results for both the 2.54 and 5.08 cm charge standoff are similar in nature in overall deformation mechanics and thus only the 5.08 cm results are presented for brevity as this charge standoff allows for a longer time period prior to correlation loss of the DIC data.

The radial displacement of the cylinders exposed to the UNDEX is characterized by an initial global deformation in the positive radial direction (away from the charge) followed by an inflection and dimpling in the center of the cylinder toward the charge location as the cylinder recovers. The upper image in Fig. 19, depicts the radial displacement of line segments along the cylinder centers for all three cylinder configurations (uncoated, thin coated and thick coated) over time. At 0.5 ms the center point displacement for the coated cylinders is 2.5 mm in the positive direction with the uncoated cylinder lagging with a center point displacement of 1.9 mm in the positive direction. Full field displacement contours over the initial 2.75 ms of the experiments can be seen in the lower portion of Fig. 19. The full field contours confirm the general shape suggested by the center line displacements.

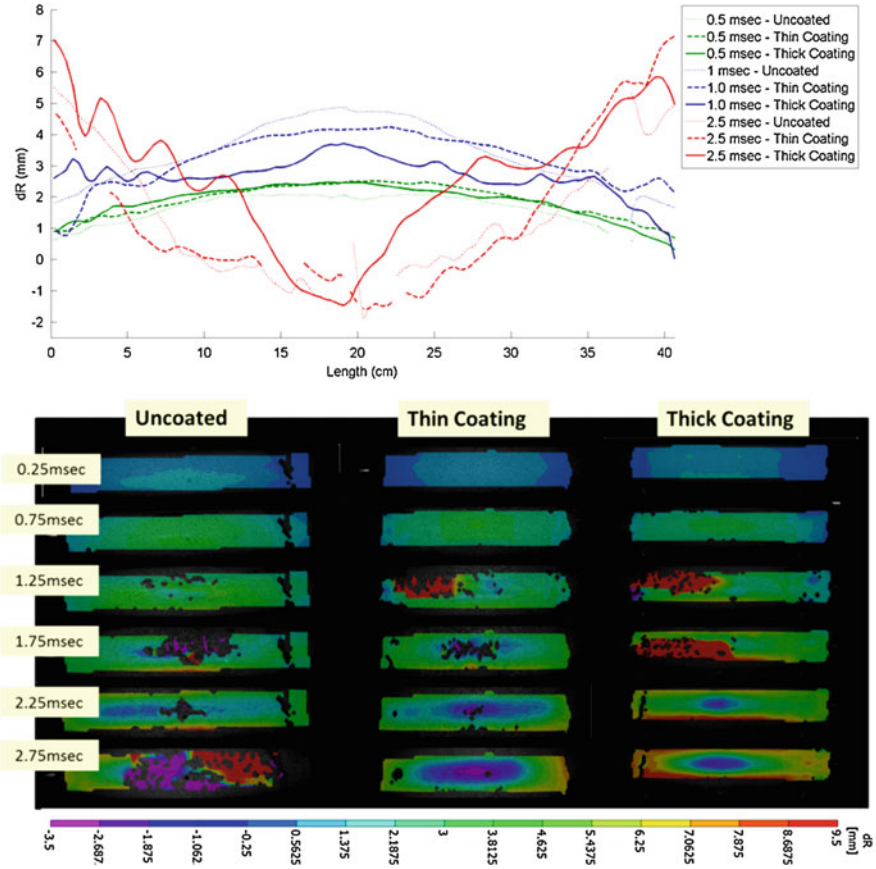

Fig. 19 Centerline and full field displacements for 5.08 cm standoff

4.3.3 Material Damage

While the application of the polyurea had minimal effect on the transient response of the cylinders, there was a significant effect of the polyurea coatings on the material damage sustained by the cylinders during the shock event. For both charge standoffs considered in the study there was a significant reduction in damage sustained with increasing coating thickness. The damage in the cylinders from the interior and exterior view are provided in Fig. 20 for the charge standoff of 2.54 cm. It is observed that the uncoated cylinder damage is dominated by large cracks and missing sections of material. Furthermore, nearest the charge location, sections of delamination can be seen along the edges of the missing portions of the cylinder. Additionally, curving cracks, suggestive of an ellipsoid indenting of the cylinder, at approximately $\pm 90^{\circ}$ from the cylinder centroid can be seen. The damage in the thinly coated cylinders is dominated by large circumferential and longitudinal cracks emanating from the point closest to the charge location. At the nexus of the

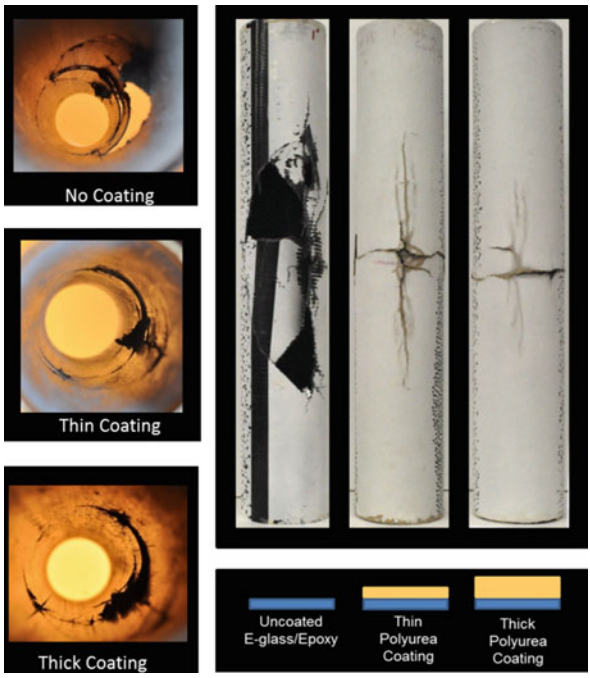

Fig. 20 Material damage for 2.54 cm charge standoff

longitudinal and circumferential cracks the damage extends through the thickness of both the composite and coating. The cylinder with the thick coating contains damage that is similar in character to that observed in the thinly coated cylinder, although at a reduced magnitude.

4.4 Computational Model Overview

The experiments which have been previously discussed, have been simulated utilizing the LS-DYNA finite element code. A fully coupled fluid structure Lagrange-Eulerian formulation is utilized due to the nature of the problem: namely highly curved wave fronts and dependence of the decay of the pressure wave during propagation through the fluid domain. This approach allows for accurate representation of the detonation of the explosive charge, resulting pressure wave propagation into the fluid, and the transient fluid structure interaction between the pressure wave and the cylinder.

The finite element model of the experiments consists of the cylinder body and endcap, polyurea coating, surrounding tank water, internal air, and the RP-503 as shown in Fig. 21. Included in the model is the ¼ representation of the system with the fluid domain extending out to a distance of 12.93 cm from the outer surface of the cylinder. The maximum charge standoff considered in the experiments was 5.08 cm,

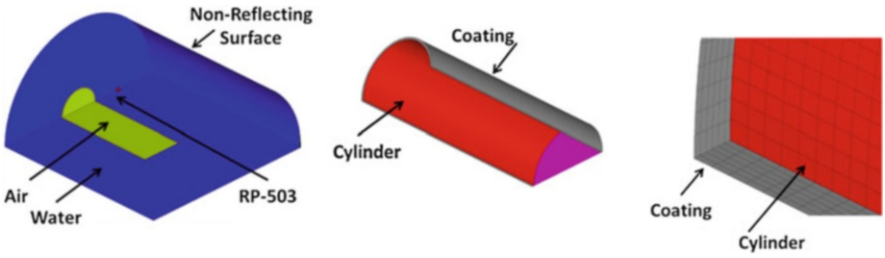

Fig. 21 Computational model detail

and thus the inclusion of the domain to a distance larger than twice the standoff value ensures boundary effects do not influence the fluid structure interaction. The Eulerian components of the coupled model consist of the water, air, and explosive charge, and are modeled with solid elements utilizing the ALE multi-material element formulation. The fluid and explosive components of the model are fully defined through the combined use of a material model and an equation of state (EOS). The structural aspect of the coupled model consists of the composite cylinder and the polyurea coating. The composite cylinder in the simulations is modeled using a single layer of shell elements with the appropriate prescribed lamina properties. Each ply is represented as having two through thickness integration points so as to capture the correct bending behavior on a per ply basis. The polyurea material is represented in the model by solid elements and are assumed to be perfectly bonded to the cylinders.

4.5 Significant Computational Results and Findings

4.5.1 Material Energy Comparisons

The internal energy of the cylinders (including coatings) during the explosive loading event is provided in Fig. 22 for the 5.08 cm charge standoff cases. The time history trends are similar in nature for the 2.54 cm charge standoff scenarios. The internal energy histories are broken down individually by the cylinder and coating, while the kinetic energies are presented as the net sum of the system. The results are presented in this manner so as to differentiate the internal energy distribution between the individual components during deformation, whereas the kinetic energy is a measure of the net motion of the system as a whole. There are several key aspects related to the energy characteristics that are illustrated by the results. It is evident that in terms of the energy experienced by the cylinder itself (internal), there is an increase as a function of coating thickness. Furthermore, for a given coating thickness it is evident that the cylinders themselves comprise ~90% of the total internal energy (cylinder plus coating) sustained with the coatings comprising 10% of the net peak energies occurring at 0.1 ms. This result is anticipated as the

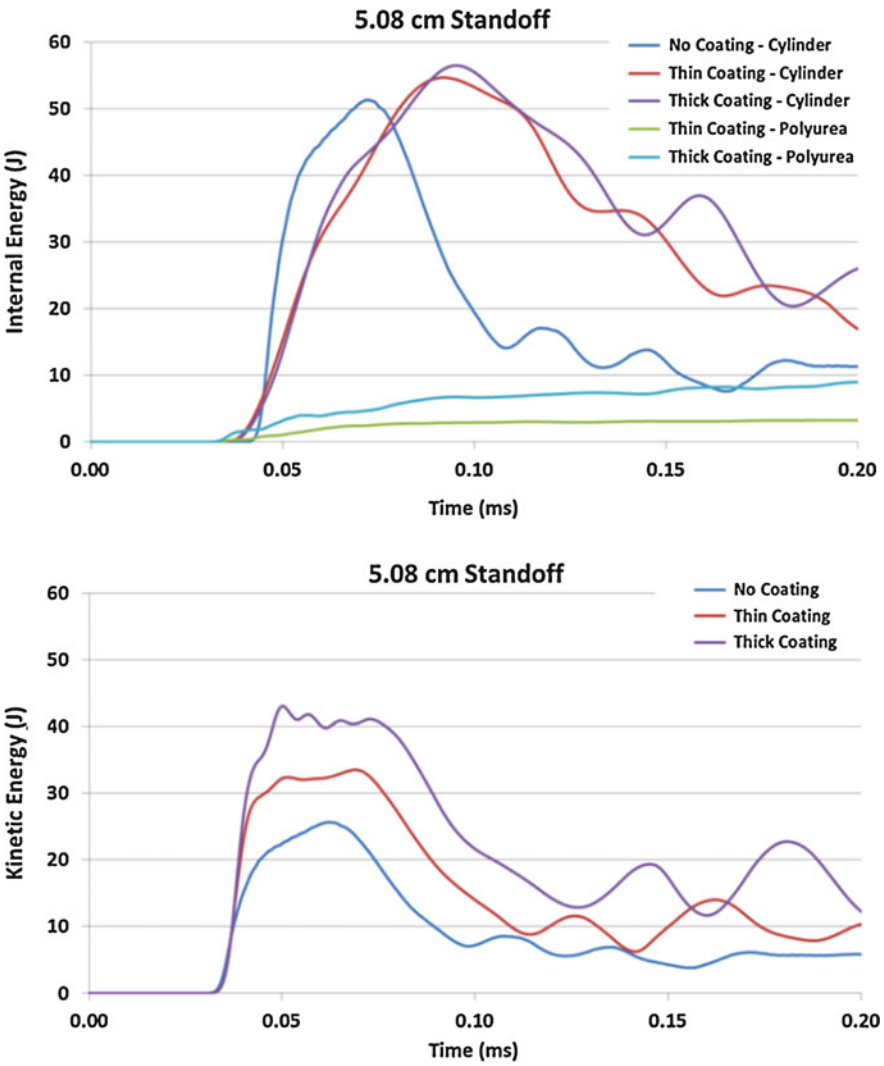

Fig. 22 Energy time histories, 5.08 cm standoff

composite material is significantly stiffer than the coating and thus for a given deformation would represent the primary load carrying mechanism. Finally, it is noted that as the coating thickness is increased there is a corresponding increase in the amount of internal energy that can be absorbed by the system (cylinder plus coating) as a whole. For the case of an uncoated cylinder, the sole mechanisms for energy absorption/dissipation are strain energy in the composite and fracture energy corresponding to the evolution of damage through fiber and matrix failure. In the presence of the coatings, there is the additional energy absorption/dissipation reservoir of the coating itself. Thus, whereas the uncoated cylinders sustain damage, the

coated cylinders can dissipate that energy into the coating itself and reduce the overall composite material loading. Hence, the coated cylinders experience higher levels of loading, but also a corresponding decrease in material damage. In terms of the internal energy observations, through comparison of the energies of the coatings themselves, the thicker coating does experience a higher level of internal energy as compared to the thin coating.

4.5.2 Strain Comparison

The strain time histories, radial and longitudinal, for the back surface of the cylinder are presented in Fig. 23 as measured on the surface of the composite cylinder itself. It is shown that the overall trends in the strain histories are consistent with those observed in the internal energy comparisons. Specifically, there is an increase in overall strain level with increasing coating thickness in both the radial and longitudinal directions. It is further noted that in observing the temporal evolution of the strains, the time to reach the peak strains is longer as the coating thickness in increased for all cases. The increase in strain as a function of increasing thickness can be attributed to the additional mass that the coatings contribute to the overall structure, while providing limited additional stiffness to the system. For the case of

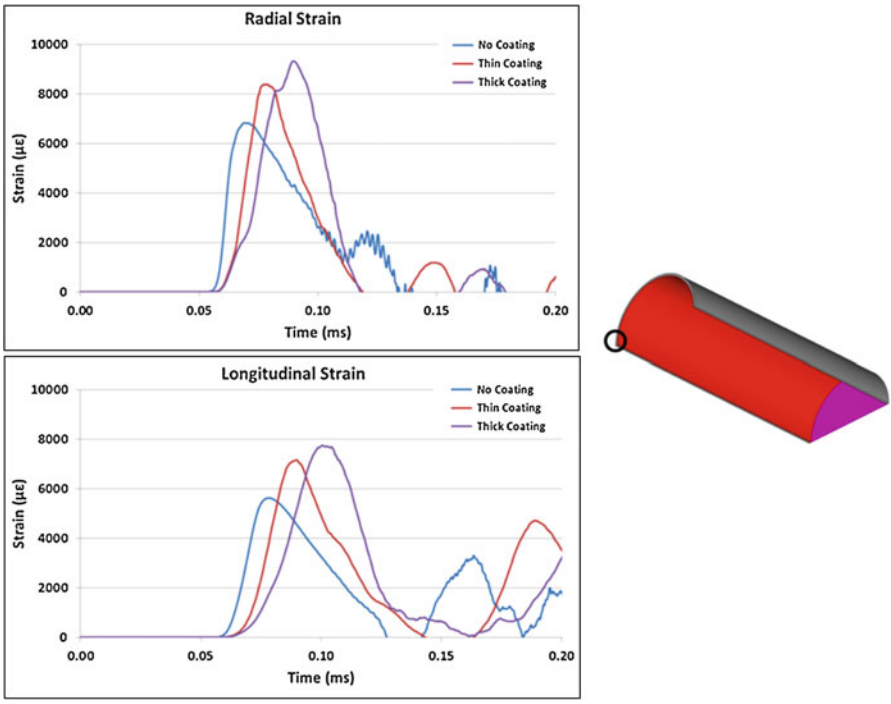

Fig. 23 Back surface strain time history, 5.08 cm charge standoff

the cylinders with a thick coating, there is an overall doubling of the structural mass of the composite/coating system. As the cylinders are accelerated and undergo deformation due to the UNDEX pressure loading, the composite cylinder is the primary load carrying mechanism due to its overall higher stiffness as compared to the coating. During this initial response the coating is adding additional mass to the system which must be arrested primarily by the composite through additional deformation which leads to resulting increases in strain. Additionally, in a similar manner as was observed with the internal energies of the system, the increase in the rear face surface strains with increasing thickness can be partially attributed to the coatings reducing or preventing the onset of material damage. The uncoated cylinders sustain significant material damage on the charge side which has the effect of dissipating a certain level of energy. By reducing the damage levels, the coating has the effect of allowing the cylinders to undergo larger overall deformations, and corresponding strains, as the energy is distributed through the system as a whole.

4.6 Results and Findings

The effects of polyurea coatings on the response and damage of submerged composite cylinders when subjected to near field UNDEX loading was investigated through experiments with corresponding computational simulations. Three unique cylinder configurations were evaluated to determine the effects of coating application and thickness The computational modeling of the experiments has been conducted with the LS-DYNA finite element code and specifically utilizes the ALE methodology so as to develop fully coupled fluid structure interaction models. The primary parameters of interest in the study are deformations, damage extents, energy levels, and material strains. The significant results of the investigation were:

1. For both the charge standoffs investigated there is a splitting of the UNDEX bubble upon interaction with the cylinders. The bubble on the non-charge side of the cylinder collapsed in close proximity to the surface of the cylinder and produced localized pressure loading on the non-charge side of the cylinder.
2. The inclusion of the polyurea coating serves to reduce the material damage levels compared to an uncoated cylinder and furthermore, damage was reduced as a function of increasing coating thickness.
3. During the transient loading of the cylinders, both the internal material energy and the overall system kinetic energy increased with increasing coating thickness. Furthermore, the composite material experiences ~90% of the overall internal energy with the coatings carrying the remaining 10%. The radial and longitudinal surface strains during the early time response of the cylinders increases with increasing coating thickness.
4. Polyurea coatings can affect structures subjected to shock loading in both beneficial and adverse means. There is an observed increase in deformation and strains with increasing coating thickness during the early time deformation, whereas there is an overall reduction in material damage and failure due to the presence of the coating over the entire time duration.

5 Weathering and Ageing Effects

Within many marine industries the use of composites is expanding to include applications which require long term and continual submergence or exposure to seawater. The deployment in such marine applications include the structures being subjected to aggressive and harsh environmental conditions, including high salinity seawater and/or salt spray that can significantly degrade their structural performance over time. These effects are of particular concern when composite vehicles are deployed in a setting where impact, shock, and blast are a concern over the period of the service life. As a result of these growing considerations there has been a body of both ongoing and recently established research investigating the manner in which composite materials with exposure to marine environments respond to dynamic loading events and how that response is adversely effected by the long term exposure. Work conducted by the authors has recently aimed at quantifying the prolonged exposure to aggressive conditions effects on the dynamic and shock response of composite materials. Accelerated ageing techniques have been developed to simulate the ageing process in a controlled laboratory environment and have been coupled with novel underwater blast loading experiments to identify the fundamental effects of ageing on structural performance.

5.1 Accelerated Ageing Method

An Accelerated Life Testing (ALT) method to simulate the long term exposure to marine environments has been implemented to investigate the effect of long term seawater submersion on the mechanical properties and shock response of a carbon fiber material. The approach utilized in the study for simulating the long term seawater immersion is to subject the material to a seawater bath at an elevated temperature. The use of the elevated temperature bath increases the rate of diffusion of the seawater into the material as compared to the absorption rate at the typical operating temperatures while also accelerating the degradation of the material. The determination of an acceleration factor, the relationship between the exposure time in the accelerated life test and an equivalent time in a typical operating environment is established. The dominant factor contributing to material degradation during prolonged submersion is fluid absorption in the matrix. In order to mathematically relate the experimental submergence of the composite plate to actual service submergence time, a water diffusion study of the matrix material has been conducted. The relationship between the accelerated life test and service time immersion is governed by the Arrhenius equation which describes the temperature dependence of the rate of reaction for a given process. The diffusion process is relatively well established and can be described by a diffusion coefficient that is a function of parameters such as temperature, type of resin and curing agent, surrounding medium composition, fillers, void content, and so on. A standard and well-accepted model for

epoxy resins, in terms of mass diffusions, is a Fickian model [44] which uses Fick's second law to predict how the concentration of a diffusive substance changes over time within a material.

The facility which has been developed to age the composite specimens is shown in Fig. 24 and allows the specimens to be submerged in a 3.5% NaCl solution (representative of sea water conditions) while also being held at an elevated temperature. The elevated temperature in the study is chosen so as to remain below the glass transition temperature of the material. Temperatures above this point would result in changes to the mechanical properties independent of the seawater ageing. The diffusion acceleration factor was determined with respect to a given temperature by conducting a water absorption evaluation performed at various temperatures; specifically: 5, 25, 45, 65, and 85 °C. Figure 25 (a) and (b) show the mass diffusion for different temperatures and the logarithmic relationship between D and E_a respectively. The diffusion coefficient was calculated from a point that is within the initial linear portion of the mass diffusion curve ($\leq$ 50% mass saturation). The diffusion coefficient was related to E_a by using Arrhenius' equation. After obtaining the activation energy for the composite material, the acceleration factor (AF) can be found as the ratio of diffusions at different temperatures as shown in Eq. (1) [45]. The submersion specimens were kept at a constant temperature ($T_1 = 338$ K), but

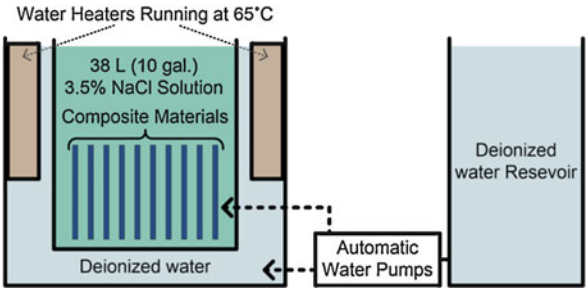

Fig. 24 Accelerated weathering facility setup

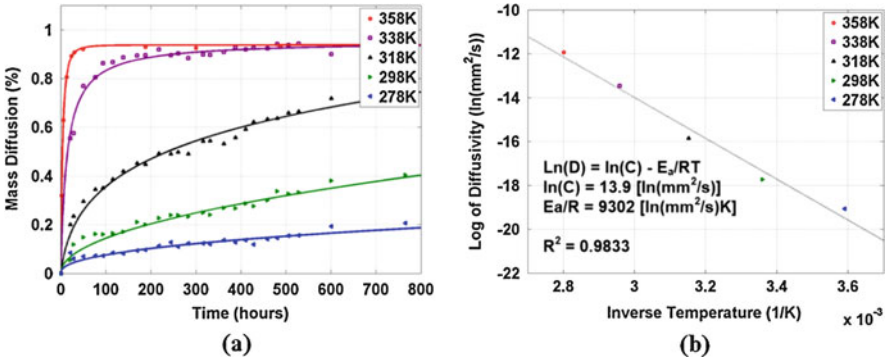

Fig. 25 (**a**) Mass diffusion and (**b**) Logarithmic relationship for diffusivity

the service temperature (T_2) can vary depending on the application. Hence, AF is application dependent. For reference, if the average ocean temperature (17 °C) is assumed to be the operational temperature, then 35 and 70 days of submersion approximates to 10 and 20 years of service respectively.

$$AF = \frac{Ce^{-\frac{E}{RT_2}}}{Ce^{-\frac{E_a}{RT_1}}} = e^{\left(\frac{E_a}{R}\right)\left(\frac{T_2 - T_1}{T_1 T_2}\right)} \quad (1)$$

5.2 Material Summary

The composite materials used in the study consist of four unidirectional carbon fiber layers with [0, 90]s and [45, −45]s layups. The laminates are manufactured from two layers of +/− 45° biaxial carbon fabric, Tenax HTS40 F13 24 K 1600tex carbon fibers with an epoxy resin matrix. Vacuum infusion was utilized in the manufacturing of all laminates plates and post curing at 70 °C for 10 h was conducted. The plates were 1.26 mm (0.050 in) in thickness. The mechanical properties as determined through ASTM standards tests is provided in Table 2 and contains both the baseline and aged properties. From the material summary it is seen that there is a general decrease in material properties with increasing submergence/exposure time, for both the moduli and strengths.

5.3 Underwater Blast Experiments

An advanced underwater blast facility is used to conduct the explosive experiments. The facility is identical to that described in Sect. 3.2 and shown in Fig. 9. The unsupported area of the panels is 254 × 254 mm^2 (10×10 in^2). An RP-503 explosive comprised of 454 mg RDX and 167 mg PETN was used as the explosive in all experiments conducted. The charge is submerged in the center of the specimens, and is placed at a 152 mm (6 in) standoff distance from the plate. The real-time response of the panels during loading is captured through the use of high speed photography

Table 2 Composite's effective mechanical properties

Weathering time (Days)	0	35	70
E_x, E_y (GPa)	78.4 +/− 1.8	78.0 +/− 2.1	74.9 +/− 2.6
V_{xy}	0.039 +/− 0.014	0.040 +/− 0.010	0.042 +/− 0.009
G_{xy} (GPa)	7.38 +/− 0.19	5.32 +/− 0.24	4.92 +/− 0.22
Yield shear stress (kPa)	36.1 +/− 1.1	25.3 +/− 1.0	21.7 +/− 0.6
Failure shear stress (kPa)	45.3 +/− 1.2	41.3 +/− 1.9	38.7 +/− 2.6

Table 3 Experimental details

Cases	Layup	Standoff distance, mm (in)	Weathering time, days (simulated years)
E45-0wd	[45,-45]s	152 (6)	0
E45-0wd-2	[45,-45]s	114 (4.5)	0
E45-0wd-3	[45,-45]s	76 (3)	0
E45-35wd	[45,-45]s	152 (6)	35 (10)
E45-70wd	[45,-45]s	152 (6)	70 (20)
E90-0wd	[0,90]s	152 (6)	0
E90-70wd	[0,90]s	152 (6)	70 (20)

coupled with digital image correlation. The two Photron SA1 high-speed cameras are used to record the shock event at 10,000 frames per second. A side view camera is also employed to capture the explosive bubble-to-structure interaction. The details of the experimental cases are summarized in Table 3.

5.4 Experimental Results

The underwater blast experiments on the composite plates are characterized by a rapid detonation of the RP-503 explosive charge, a high pressure/short duration pressure loading, and a subsequent longer duration growth of the UNDEX bubble. These characteristics are highlighted in the high speed side-view images in Fig. 26. From the images it is also seen that due to the relatively small standoff of the charge to the plate as compared to the maximum bubble size there is a physical interaction between the bubble and the plate itself. The high pressures characteristic of an underwater explosion are also shown in Fig. 26 as recorded at varying standoffs from the charge location. The shock from the explosive is distinguished by an immediate rise in pressure followed by exponential decay. The amplitude of the explosive pressure decreases spherically by 1/R from the explosive location. From the pressure time histories it is observed that the pressures from the explosive detonation are very large, 20–30 MPa, but also very short in duration, less than 0.25 ms from peak to full decay.

The center-point out of plane deformation of the 45/−45 and 0/90 panels with a charge standoff of 152 mm are provided in Fig. 27. The deformation evolution is highlighted by the following trend: (1) A flexure towards the air side during the initial pressure loading phase upto a maximum displacement value, (2) a rebound phase during the surface cavitation (at vacuum pressure) with a rapid flexure towards the water-side of the plate to a magnitude beyond its initial displacement, and finally, (3) an abrupt increase in displacement towards the air side of the plate due to the cavition bubble collapse. Furthermore, the ageing of the plates led to an increase in maximum displacements for the same loading condition as highlighted in the time histories. After weathering the [45,-45]s composite for 35 days, the maximum center point displacements increase by an average of 20%. An additional 5% increase in

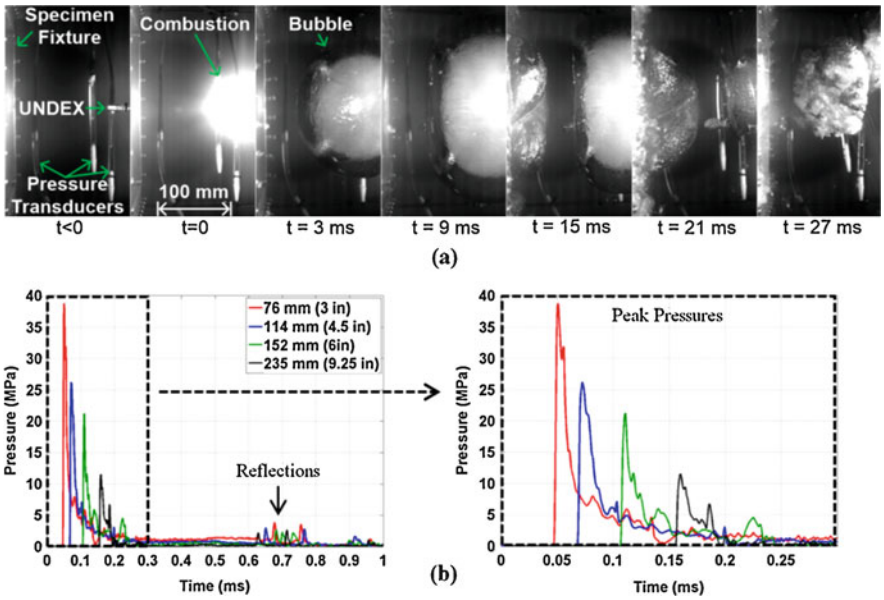

Fig. 26 (**a**) Fluid-structure interaction images, (**b**) Pressure history from the explosive

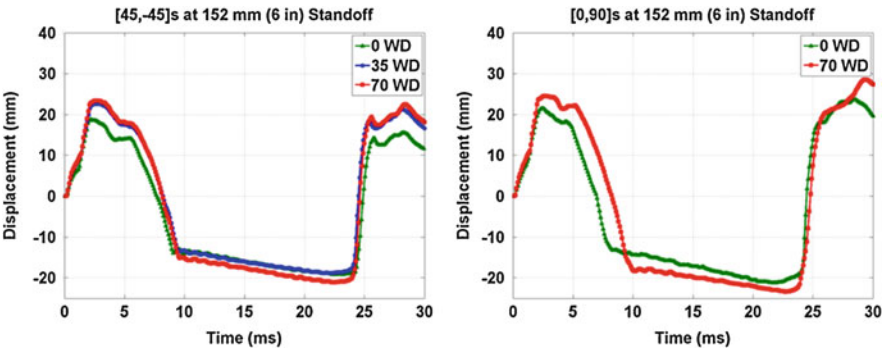

Fig. 27 Center point displacements for [45,-45]s and [0,90]s weathered composites

displacement is seen for the 70 weathering days (WD) cases indicating further material degradation. Furthermore, a post mortem evaluation of the panels to investigate the material damage characteristics was performed. The analysis revealed that damage increased with weathering time. Damage observed in the [45,-45]s cases consisted primarily of through-thickness damage near the plate's corners as illustrated in Fig. 28. Additionally, in terms of the 35 WD and 70 WD, there is a notable increase in average crack length. This increase in crack length suggests further material degradation from fiber/matrix debonding after saturation. A similar trend in increasing damage with ageing time was seen in the [0,90]s laminate cases,

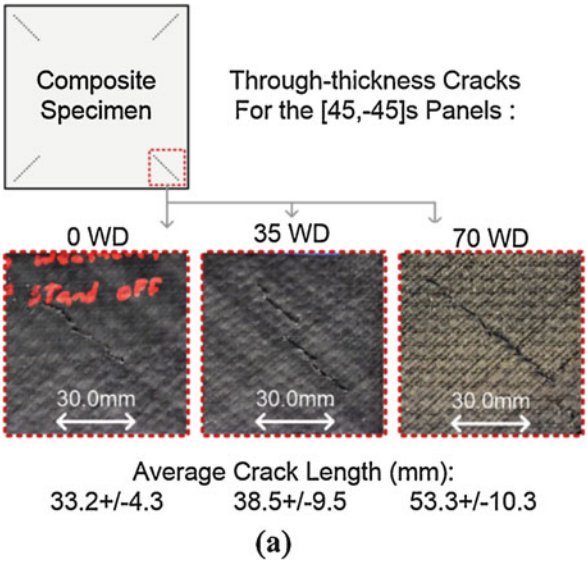

Fig. 28 Interfibrillar and through-thickness cracking for the [45,-45]s cases

although the damage was predominately seen in the form of delamination near its corners rather than cracking. The difference in damage between [45,-45]s and [0,90]s arises from how the boundary interacts with the fiber orientations.

5.5 Significant Findings

A detailed experimental investigation into the effects of long term seawater immersion on the mechanical and shock response of carbon fiber laminates was conducted. The significant findings of the study are:

1. There is a measurable degradation of the mechanical properties of the laminates as a result of the seawater submersion. The shear properties, which are primarily governed by the epoxy matrix exhibited the largest degradation.
2. The peak center point displacements during shock loading increased with ageing time, namely for the 35 day weathering period of both the laminate constructions considered. The additional weathering time of 70 days had only a minor additional effect.
3. The length of weathering time in seawater is also related to the amount of accumulated damage sustained by the plates during loading. In the 45/−45 plates there was an increase in through-thickness cracking whereas in the 0/90 laminates the delamination levels increased.

6 Conclusion

Composite material systems are increasingly being considered for the design and construction of advanced structures and vehicles. The materials are able to meet the competing design interests of increased stiffness and strength with decreased overall weight as well as ease of manufacture and decreased maintenance requirements. As a result of the performance increases afforded by these materials they are being increasingly employed in applications pertaining to aerospace, marine, infrastructure, and defense. As these materials find wider application consideration must also be given to the extreme loading conditions which are imparted to them in the expected operating theatres, including shock, blast, and environmental exposure. It is with these considerations in mind that the research program discussed in the preceding sections has been undertaken and continues. The early part of the program investigated the response of composite plates to far-field underwater explosive conditions and subsequently transitioned to the study of near field blast loading. More recently the complex interactions between near field pressure waves and cylindrical geometries was considered, including bubble interaction phenomena. Furthermore, the degrading effects of long term submersion in a salt water environment on mechanical performance was investigated. Each of the components of the program have developed and utilized both advanced experimental techniques with detailed numerical modeling approaches. The significant findings from the research are:

1. The fluid structure interactions resulting from the impingement of an UNDEX pressure wave (near or far field) on a nearby composite structure are complex, both temporally and spatially. That complexity translates to the bubble-structure interaction as well for near-field explosions.
2. The application of rate-dependent, elastomeric coatings, namely polyurea, can be beneficial during loading of a structure in terms of both transient deflection reduction and, more importantly, as a damage mitigation and/or reduction method.
3. Long term seawater submersion has a degrading effect on the mechanical performance of the materials considered with reductions in both modulus and strength observed. Additionally, increased damage levels with increased ageing were noted.
4. Numerical/computational models can be employed to accurately simulate the complex fluid structure interactions, transient responses, and damage levels as compared to the corresponding experiments.

Acknowledgments The work was supported by the Office of Naval Research under the Solid Mechanics Program managed by Dr. Y.D.S. Rajapakse and by the Naval Undersea Warfare Center Division Newport In-House Laboratory Independent Research Program (Chief Technology Office) and Internal Investment Program (Strategic Investment Office).

References

1. Nurick G, Olson M, Fagnan J, Levin A (1995) Deformation and tearing of blast loaded Stiffened Square plates. Int J Impact Eng 16:273–291
2. Nurick G, Shave G (1996) The deformation and tearing of Thin Square plates subjected to impulsive loads–an experimental study. Int J Impact Eng 18:99–116
3. Tekalur AS, Shivakumar K, Shukla A (2008) Mechanical behavior and damage evolution in E-glass vinyl Ester and Carbon composites subjected to static and blast loads. Compos Part B 39:57–65
4. Mouritz AP (2001) Ballistic impact and explosive blast resistance of stitched composites. Compos Part B 32:431–439
5. Mourtiz AP (1996) The effect of underwater explosion shock loading on the flexural properties of GRP laminates. Int J Impact Eng 18:129–139
6. Mouritz AP (1995) The effect of underwater explosion shock loading on the fatigue behavior of GRP laminates. Compos 26:3–9
7. Dear J, Brown S (2003) Impact damage processes in reinforced polymeric materials. Compos A: Appl Sci Manuf 34:411–420
8. Franz T, Nurick G, Perry M (2002) Experimental investigation into the response of chopped-strand mat glassfibre laminates to blast loading. Int J Impact Load 27:639–667
9. LeBlanc J, Shukla A, Rousseau C, Bogdanovich A (2007) Shock loading of three-dimensional woven composite materials. Compos Struct 79:344–355
10. LeBlanc J, Shukla A (2010) Dynamic response and damage evolution in composite materials subjected to underwater explosive loading: an experimental and computational study. Compos Struct 92:2421–2430
11. LeBlanc J, Shukla A (2011) Dynamic response of curved composite plates to underwater explosive loading: experimental and computational comparisons. Compos Struct 93:3072–3081
12. Jackson M, Shukla A (2010) Performance of Sandwich composites subjected to sequential impact and air blast loading. Compos Part B 42:155–166. https://doi.org/10.1016/j.compositesb.2010.09.005
13. Schubel PM, Luo J, Daniel I (2007) Impact and post impact behavior of composite Sandwich panels. Compos Part A 38:1051–1057
14. Arora H, Hooper P, Dear JP (2010) Impact and blast resistance of glass fibre reinforced Sandwich composite materials. In: Proceedings of IMPLAST 2010
15. Avachat S, Zhou M (2014) Response of cylindrical composite structures to underwater impulsive loading. Procedia Eng 88:69–76
16. Avachat S, Zhou M (2015) High-speed digital imaging and computational modeling of dynamic failure in composite structures subjected to underwater impulsive loads. Int J Impact Eng 77:147–165
17. Latourte F, Gregoire D, Zenkert D, Wei X, Espinosa H (2011) Failure mechanisms in composite plates subjected to underwater impulsive loads. J Mech Phys Solids 59:1623–1646
18. Espinosa H, Lee S, Moldovan N (2006) A novel fluid structure interaction experiment to investigate deformation of structural elements subjected to impulsive loading. Exp Mech 46 (6):805–824
19. Matzenmiller A, Lubliner J, Taylor RL (1995) A constitutive model for anisotropic damage in fiber-composites. Mech Mater 20:125–152
20. Zako M, Uetsuji Y, Kurashiki T (2003) Finite element analysis of damaged woven fabric composite materials. Compos Sci Technol 63:507–516
21. Dyka CT, Badaliance R (1998) Damage in marine composites caused by shock loading. Compos Sci Technol 58:1433–1442
22. O'Daniel JL, Koudela KL, Krauthammer T (2005) Numerical simulation and validation of distributed impact events. Int J Impact Eng 31:1013–1038

23. McGregor CJ, Vaziri R, Poursartip A, Xiao X (2007) Simulation of progressive damage development in braided composite tubes under axial compression. Compos Part A 38:2247–2259
24. Gama B, Xiao J, Haque M, Yen C, Gillespie J (2004) Experimental and numerical investigations on damage and delamination in thick plain weave S-2 glass composites under quasi-static punch shear loading. Center for Composite Materials, University of Delaware
25. Donadon MV, Iannucci L, Falzon BG, Hodgkinson JM, de Almeida SFM (2008) A progressive failure model for composite laminates subjected to low velocity impact damage. Comput Struct 86:1232–1252
26. Hosseinzadeh R, Shokrieh MM, Lessard L (2006) Damage behavior of Fiber reinforced composite plates subjected to drop weight impacts. Compos Sci Technol 66:61–68
27. Tagarielli VL, Deshpande VS, Fleck NA (2010) Prediction of the dynamic response of composite Sandwich beams under shock loading. Int J Impact Eng 37:854–864
28. Batra RC, Hassan NM (2007) Response of Fiber reinforced composites to underwater explosive loads. Compos Part B 38:448–468
29. Davies P (2016) Environmental degradation of composites for marine structures: new materials and new applications. Phil Trans Math Phys Eng Sci 374(2071):20150272. https://doi.org/10.1098/rsta.2015.0272
30. Shirrell C, Halpin J (1977) Moisture absorption and desorption in epoxy composite laminates. Compos mater: testing and design (Fourth Conference). https://doi.org/10.1520/stp26963s
31. Browning C, Husman G, Whitney J (1977) Moisture effects in epoxy matrix composites. In: Davis J (ed) Composite materials: testing and design (Fourth Conference), STP26961S. ASTM International, West Conshohocken, pp 481–496. https://doi.org/10.1520/STP26961S
32. Blikstad M, Sjoblom PO, Johannesson TR (1984) Long-term moisture absorption in graphite/epoxy angle-ply laminates. J Compos Mater 18(1):32–46. https://doi.org/10.1177/002199838401800103
33. Neumann S, Marom G (1987) Prediction of moisture diffusion parameters in composite materials under stress. J Compos Mater 21(1):68–80. https://doi.org/10.1177/002199838702100105
34. Choqueuse D, Davies P (2008) Aging of composites in underwater applications. Ageing of Composites. https://doi.org/10.1201/9781439832493.ch18
35. Sar B, Fréour S, Davies P, Jacquemin F (2012) Coupling moisture diffusion and internal mechanical states in polymers – a thermodynamical approach. Eur J Mech A Solid 36:38–43. https://doi.org/10.1016/j.euromechsol.2012.02.009
36. Fichera M, Totten K, Carlsson LA (2015) Seawater effects on transverse tensile strength of carbon/vinyl ester as determined from single-fiber and macroscopic specimens. J Mater Sci 50 (22):7248–7261. https://doi.org/10.1007/s10853-015-9279-3
37. Choqueuse D, Davies P, Mazéas F, Baizeau R (1997) Aging of composites in water: comparison of five materials in terms of absorption kinetics and evolution of mechanical properties. In: High temperature and environmental effects on polymeric composites, vol 2. https://doi.org/10.1520/stp11369s
38. Davies P, Rajapakse Y (2014) Durability of composites in a marine environment. Springer, Dordrecht
39. Crank J (1975) The mathematics of diffusion, 2nd edn. Oxford University Press, London
40. Shillings C, Javier C, LeBlanc J, Tilton C, Corverse L, Shukla A (Submitted 2017) Experimental and computational investigation of blast response of Carbon-Epoxy weathered composite materials. Composites B
41. Poche L, Zalesak J (1992) Development of a water-filled conical shock tube for shock testing of small sonar transducers by simulation of the test conditions for the heavyweight MIL-S-901D (Navy). NRL Memorandum Report 7109
42. Coombs A, Thornhill CK (1967) An underwater explosive shock gun. J Fluid Mech 29:373–383

43. Filler WS (1964) Propagation of shock waves in a hydrodynamic conical shock tube. Phys Fluids 7:664–667
44. Popineau S, Rondeau-Mouro C, Sulpice-Gaillet C, Shanahan ME (2005) Free/bound water absorption in an epoxy adhesive. Polymer 46(24):10733–10740. https://doi.org/10.1016/j.polymer.2005.09.008
45. Rice M (2011) Activation energy calculation for the diffusion of water into PR-1590 and Pellethane 2103-80AW polyurethanes. NUWC-NPT Technical Memo 11–062